Universitatea Naţională de Ştiinţă şi Tehnologie POLITEHNICA BUCUREŞTI

DOCTORAL SCHOOL
MATERIALS SCIENCE AND ENGINEERING

313 Splaiul Independţei, Sector 6, Bucharest, 060042
Phone/fax: 021 402 9624; http://www.sdsim.upb.ro

PhD Thesis Summary

Research on the influence of acetate-based composite coatings of cellulose on the biodegradation of Mg3Nd type magnesium alloys

---

Doctoral student: Engineer ALEXANDRU V. STREZA

PhD supervisor: Prof. Univ. Skilled. Dr. Eng. ANTONIAC VASILE IULIAN

DOCTORAL COMMITTEE

chairman	**Prof. Eng. Ghiban Brândușa**	**National University of Science and Polytechnic Technology Bucharest**
Conductor of PHD	**Prof. Habil. Univ. Dr. Eng. ANTONIAC Vasile Iulian**	**National University of Science and Polytechnic Technology Bucharest**
Reviewers SCIENTIFIC	**Prof. Dr. Med. Ciocan Toma Lucian**	**The University of Medicine and Pharmacy "Carol Davila" Bucharest**
	Prof. Dr. Eng. Popescu Violeta	**Technical University of Cluj Napoca**
	Prof. Dr. Eng. Predescu Cristian	**National University of Science and Polytechnic Technology Bucharest**

Bucharest 2023

content

Thanks

This thesis could not have been completed without the help, support, guidance and understanding of some people who, through their way of being, contributed to my formation as a person and created new role models for me. First of all, I want to thank the scientific supervisor of this doctoral thesis, Mr. Prof.Univ.Habil.Dr.Ing. Vasile-Iulian Antoniac from the National University of Science and Technology POLITEHNICA Bucharest, for the trust, professionalism and scientific quality offered, but above all for the time, patience, understanding and last but not least the friendship he showed.

I thank the doctoral committee members, respectively Prof.Dr.Med. Ciocan Toma Lucian from the University of Medicine and Pharmacy Carol-Davila Bucharest, Prof.Dr.Ing. Violeta Popescu from the Technical University of Cluj-Napoca, Prof.Dr.Ing. Cristian Predescu from the National University of Science and Technology POLITEHNICA Bucharest, for the time given to the evaluation of the doctoral thesis.

I also thank the members of the doctoral guidance committee, respectively Prof.Habil.Dr.Ing. Marian Miculescu, Prof. Dr. Eng. Brânduța Ghiban, Ș.L.Dr.Ing. Octavian Trante, for the time allocated and the useful suggestions received throughout the doctoral internship. Last but not least, I also thank the director of SDSIM, Prof.Habil.Dr.Ing. Florin Miculescu, for the technical support provided.

This doctoral thesis would not have been complete without the significant help of teaching staff from the National University of Science and Technology POLITEHNICA Bucharest, namely Prof.Habil.Dr.Ing. Marian Miculescu, Prof.Habil.Dr.Ing. Ștefan-Ioan Voicu, Prof.Habil.Dr.Ing. Florin Miculescu, Prof. Dr. Eng. Cosmin-Mihai Cotruț, SLDr.Ing. Robert Ciocoiu, SLDr. Eng. Alina Robu; University of Medicine and Pharmacy in Craiova - Prof.Dr.Med. Horia Manolea and the University of Medicine and Pharmacy Gr.T.Popa Iași - Prof.Dr.Med. Liliana Vereștiuc, to whom I thank both for their time and help, as well as for the fruitful scientific discussions.

I also thank Ms. CSIII. Aurora Antoniac, from the National University of Science and Technology POLITEHNICA Bucharest for the permanent guidance and scientific advice, but especially for the patience shown during the realization of this doctoral thesis, thus contributing to my professional training and as a person.

I would like to thank my parents, Maria Streza and Vasile Streza, who throughout of time guided my steps in life, and who instilled in me the desire to know, to improve myself, to learn new things, and to climb a little higher.

Thanks to all fellow PhD students and teaching staff from the Department of Metallic Materials Science, Physical Metallurgy, Faculty of Materials Science and Engineering, POLITEHNICA Bucharest National University of Science and Technology, who encouraged and supported me constantly in my scientific activities.

With special gratitude and love, I dedicate this thesis to my wife Elena Streza and my son Eduard Streza, who were by my side, showed me their affection, but above all, they were patient with me. I thank everyone who had the patience to read and correct this thesis and who helped me throughout my doctoral internship.

With consideration,
Stresa Alexandru

SUMMARY

The present doctoral thesis includes both a theoretical study and a series of own experimental research carried out with the aim of characterizing and testing two experimental magnesium alloys of the Mg3Nd type, with a small variable content of other elements, potentially usable in the execution of orthopedic implants .

Magnesium-based metal alloys currently represent the new generation of biodegradable metal materials with good osseointegration properties. The main limitation of magnesium alloys is the release of hydrogen at the tissue level and too rapid degradation, thus requiring the correlation of the speed and rate of corrosion with the repair process of the damaged bone tissue. Therefore, in such applications it is necessary to improve the corrosion resistance of magnesium alloys, which is possible by using bioceramic, polymer or composite coatings.

The use of these coatings also helps in better osseointegration in the case of orthopedic implants. The main objective of the experimental research carried out within the present doctoral thesis was to evaluate the influence of composite coatings based on cellulose acetate, reinforced with magnesium particles, respectively with hydroxyapatite particles, on the biodegradation of Mg3Nd type magnesium alloys.

The potential of these innovative magnesium alloys, of the Mg3Nd type, to be usable in the execution of orthopedic implants was also investigated.

A complex microstructural characterization of the experimental magnesium alloys was performed using optical microscopy, X-ray diffraction and scanning electron microscopy. For functional testing, corrosion resistance determinations in simulated environments and in vitro and in vivo biocompatibility tests were performed on both coatings and experimental magnesium Mg3Nd alloys before and after coating with composite materials.

In conclusion, the experimental results obtained demonstrated the fact that the experimental Mg3Nd magnesium alloys, after coating with composite materials based on cellulose acetate, reinforced with magnesium particles, respectively with hydroxyapatite particles, proved to be biocompatible as a result of biocompatibility tests *in vivo* carried out on laboratory rats, and have a biodegradation rate favorable for use in the execution of orthopedic implants.

Keywords:
magnesium alloys, Mg3Nd, composites, cellulose acetate, coatings, biodegradation.

THEORETICAL PART

CHAPTER 1. THE CURRENT STAGE OF RESEARCH ON MAGNESIUM ALLOYS USABLE AS IMPLANT MATERIALS

To date, different categories of medical devices are produced using different manufacturing systems, but the main challenge for materials engineering is the appropriate choice of materials for the production of these implantable medical devices.

For this purpose, different types of materials such as natural or synthetic polymers, ceramics, metals, composites and hydrogels have been used to observe the differences between them. Furthermore, when planning or determining the suitability of a sample, it is important to assess whether it meets the following key requirements: biocompatibility, bioactivity and biodegradability.

Biocompatibility represents the complex of phenomena that occur when biomaterials, in the form of medical devices, interact with living tissues. Also, biocompatibility defines the property of a material to be compatible with living organisms, i.e. to be accepted by the body in its entirety, without generating adverse reactions [2]. This is an essential criterion that must be fulfilled by any device with an application in the medical field.

Bioactivity is the ability of a biomaterial to interact with tissue surrounding, ensuring cell adhesion, proliferation and differentiation. In general, materials that are formed from trace elements existing in the human body have greater bioactivity and can promote cellular recognition by evoking the specific cellular response to support tissue growth. To this end, it is possible to modify the surface of the biomaterial by adding an extracellular matrix of collagen, fibronectin and laminin macromolecules, to produce a biomimetic environment equivalent to the native tissue capable of influencing cellular behavior.

Fe (pure Fe, Fe-Mn alloys) and magnesium (Mg – Mg-Ca, Mg-Ca-Zn, Mg-Ca-Zr alloys) belong to the category of biodegradable metallic biomaterials, which are recommended for medical applications in the cardiovascular field (coronary stents) or orthopedic (bone fixation plates and screws, centromedullary rods). Biodegradable metals must provide adequate mechanical support to support the healing process during the implantation period, but it is difficult to define a period of implant support activity as close as possible to medical reality. It is noted that the design strategy of some biodegradable metallic implants made of Fe or Mg-based alloys must address both the problem of degradation speed and the increase of mechanical properties by changing the chemical composition and microstructural characteristics.

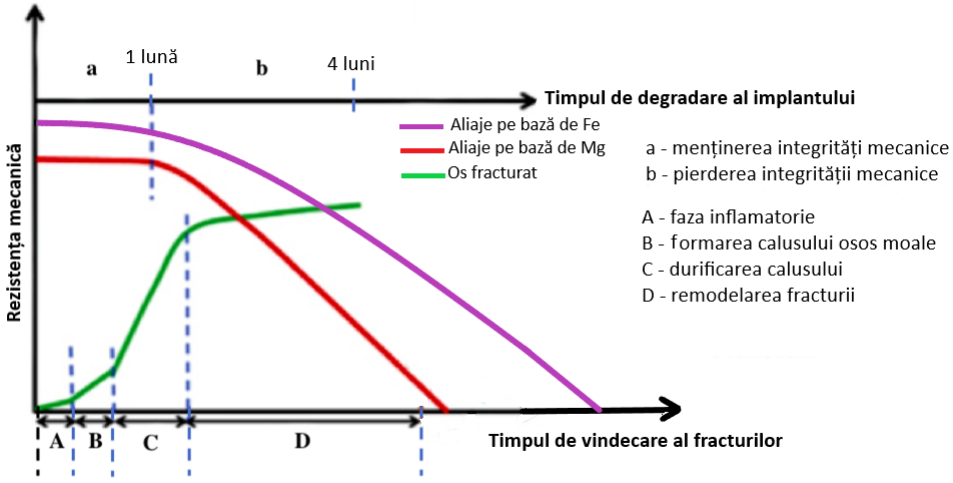

Figure1.1. Correlation between degradation of biodegradable implants and fracture repair (case ideal) [7]

The performance of materials in the human body can be classified in many ways, but a biomaterial is used to achieve the functioning of medical devices in a safe, reliable, economic and physiologically accepted manner. Biomaterials have widespread applicability in the field of regenerative medicine, and the following table exemplifies the destination, functions and role for which they are developed depending on the scope of activity [5,9].

The major disadvantage of using Mg in many engineering applications is its low corrosion resistance, especially in electrolytic environments, where it degrades rapidly. When pure, chemically unprotected magnesium is exposed to moist atmospheric air, it develops a thick amorphous layer consisting of magnesium hydroxide ($Mg(OH)_2$). The oxidation rate of this protective layer is typically about 0.01 mm/year, while the oxidation rate in salt water is about 0.30 mm/year [30].

The real cause of corrosion processes lies in the thermodynamic instability of metals that tend to return to their original state of metallic compounds. Because of their structure characterized by the presence of free electrons in the crystal network, metallic materials react extremely easily with the usual aqueous environments, therefore also with biological ones, being altered by corrosion from these environments [31].

Corrosion in the biological environment is more complex than that in industrial environments, because the rate of corrosion is influenced by several factors, such as: pH of body fluids and its variations, ion concentration, presence of proteins and protein adsorption on the implant, reactions that occur between the biological environment and the metallic material; the existence of static or dynamic demands. In any degradation process, the presence of static or cyclic stresses can accelerate these processes [2].

The corrosion of magnesium in the physiological environment can be expressed within the following equations [1.3]:

anodic reaction: $Mg \rightarrow Mg^{2-} + 2e^-$ (1.1)

cathodic reaction: $2H_2O + 2e^- \rightarrow 2OH^- + H_2$ (1.2)

The general reaction of the corrosion process is shown in the following equation:

$Mg_{(s)} + 2H_2A_{(it)} \rightarrow Mg(OH)_{2\,(s)} + H_{2\,(g)}$ (1.3)

Another undesirable consequence of the corrosion process in magnesium alloys is the formation of hydrogen bubbles due to the chloride-rich environment, which generally appear in the first week after surgery, then disappear after 2 - 3 weeks. It has been shown that if the corrosion rate of Mg can be controlled so that the hydrogen evolution rate is below 0.01 ml/cm_2 per day, the implant will not pose a threat from this point of view.

The corrosive process of Mg in the body is a complex phenomenon, and the main corrosion products are hydrogen gas and $Mg(OH)_2$. When $Mg(OH)_2$under standard environmental conditions, it forms a partially protective layer on the surface of Mg alloys. Rapid dissolution of the Mg substrate generating H $gas_2$and HO ions-[35–37].

In addition, there is increasing evidence that the oxygen reduction reaction (ORR) occurs in this process (equation 1.4).

$Mgr_{(s)} + 2H_2A_{(it)} + Oh_{2(g)} \rightarrow 2Mg(OH)_{2(s)}$ (1.4)

This reaction is not reflected in the total process of cathodic corrosion of Mg, although it can be used to compare the corrosion resistance of Mg alloys with similar degradation values.

Reactions of the Mg solid layer and the Mg(OH) surface $layer_2$with chlorine ions in the aqueous medium are presented in the following equations [38]:

$Mgr_{(s)} + 2Cl^-_{\,(that)} \rightarrow MgCl_2 + 2e^-$ (1.5)

$Mg(OH)_{2(s)} + 2Cl^-_{\,(that)} \rightarrow MgCl_2 + 2OH^-$ (1.6)

Thus, magnesium breaks down into Mg ions^{2+}, which dissolves and reacts with water. In the following the reactions, hydroxyl groups are created and hydrogen bubbles are generated, which have the secondary effect of increasing the local pH in the body. High pH inhibits cell proliferation and tissue formation. In a static solution, the pH can rise as high as ten. During corrosion, for pure Mg, 1 ml of H is dissolved$_2$for every 1 mg of dissolved Mg. Mgr^{2+}reacts with hydroxyl groups (HO$^-$) and precipitates as magnesium hydroxide (Mg(OH)$_2$). At the same time, a passive intermediate layer of Mg hydroxide or Mg oxide (MgO) is formed on the degradation surface [39].

CHAPTER 2. *COATINGS FOR DEGRADATION CONTROL OF MAGNESIUM ALLOYS USED AS IMPLANT MATERIALS*

Numerous researches have shown that surface modifications, such as polishing, oxidation, passivation, ion implantation, coatings, have a considerable influence on the properties and functional activity of an implantable biomaterial. These techniques improve the biocompatibility and osseointegration of metal implants. The mechanical properties of the substrate are usually maintained after surface modification. Coatings are used to minimize localized corrosion of magnesium and its alloys, especially in the initial stage after implantation. Since the coating is temporary, they can gradually dissolve in vivo without producing harmful effects on the surrounding tissues [75].

In general, the principle of modifying the surface of magnesium alloys seems relatively simple, because it involves preventing direct contact between the magnesium alloy substrate and the human environment, so that corrosion phenomena are inhibited or delayed.

*Conversion covers*are made*in situ*, through reactions that take place between the base material and the environment (intracellular). Usually, the substrate surfaces are converted during the chemical or electrochemical process into an oxide layer. Relative to the original metal surface, the oxide layer grows inside and outside at the same level and therefore the geometry of the component changes. The layers produced are inorganic and have a ceramic character

*Deposit coverages*they can be obtained using very diverse physical and chemical methods; the coating techniques used are closely related to the coating materials. However, for Mg alloys, in the case of applying an organic coating, due to the high alkalinity of the surface, a special surface treatment is required [77,79].

Another general classification of coating methods involves dividing them into dry (vacuum) and wet (solution) methods. Dry methods are classified into two categories: physical vapor deposition (PVD) in vacuum and plasma and chemical vapor deposition (CVD) methods. Wet methods are chemical deposition methods from solutions, such as sol-gel, chemical or polyelectrolytic self-assembly, electrochemical deposition.

PART II – EXPERIMENTAL PART *CHAPTER 3. RESEARCH METHODOLOGY*

3.1. The purpose of the work, the experimental materials and the work plan

The main objective of the experimental research carried out in the framework of this doctoral thesis was to evaluate the influence of composite coatings based on cellulose acetate, reinforced with magnesium powder, respectively with hydroxyapatite powder, on the biodegradation of Mg3Nd type magnesium alloys.

During the development of the thesis, other objectives were pursued, such as the determination of the influence of the reinforcing elements on the morpho-structural characteristics and functional properties of the experimental composite coatings, the evaluation of the effect induced by each type of coating on the biodegradation and biocompatibility of magnesium alloys from the Mg3Nd system, with

the purpose of meeting the functional requirements imposed by their use in the execution of temporary orthopedic implants.

In order to achieve the main objective of this work, several steps were taken stages:

- ➢ Selection of the system of magnesium alloys potentially usable in the execution of temporary orthopedic implants based on specific criteria of biofunctionality, respectively of the experimental magnesium alloys Mg3Nd_A and Mg2Nd_B;
- ➢ Selection of the optimal method of surface modification of the experimental magnesium alloys Mg3Nd_A and Mg2Nd_B, respectively by immersion in polymer solutions of cellulose acetate and composites with polymer matrix of cellulose acetate reinforced with magnesium and hydroxyapatite powder;
- ➢ Complex microstructural characterization of alloys from the Mg3Nd system, respectively Mg3Nd_A and Mg3Md_B;
- ➢ Deposition of composite polymer coatings with cellulose acetate polymer matrix reinforced with magnesium powder and hydroxyapatite on the surface of experimental magnesium alloys Mg3Nd_A and Mg3Md_B;
- ➢ Characterization of composite polymer coatings with cellulose acetate polymer matrix reinforced with magnesium powder and hydroxyapatite by:
  - aDemonstration of the functionality of composite coatings by determining the rate of swelling, degradation rate in PBS solution;
  - aDemonstration of the functionality of composite polymer coatings by performing some biocompatibility tests*in vitro* on cell cultures; a
  - Surface characterization of coated Mg3Nd alloys;
  - aDemonstration of the functionality of coated and uncoated Mg3Nd alloys by determination of the amount of hydrogen released and the loss of mass by immersion tests;
  - aDemonstration of the functionality of coated and uncoated Mg3Nd alloys by performing some electrochemical corrosion tests;\
  - aDemonstration of the functionality of coated and uncoated Mg3Nd alloys by performing biocompatibility tests*in vivo* on laboratory rats, Whistar breed. The experimental materials that were used in this doctoral thesis are:
- ➢ Mg3Nd magnesium alloys with variable Yttrium (Y) content, coded Mg3Nd_A and Mg3Nd_B, obtained at the Dead Sea Magnesium Company (Beersheva, Israel) using the gravity casting method in crucibles or sand molds.

  In order to characterize, test and demonstrate the functionality of the obtained Mg3Nd alloys, metallographic samples with dimensions of 15×15×5 mm were made and prepared$_3$(width×length×height).
- ➢ Cellulose acetate (CA, 30% degree of acetylation, Sigma-Aldrich, St. Louis, MO, USA), N,N'-dimethyl formamide (DMF, Sigma-Aldrich, St. Louis, MO, USA), particles of hydroxyapatite (granulation 200 nm, Sigma-Aldrich, St. Louis, MO, USA) and magnesium particles (purity 99%, granulation ~ 50 μm, STREM CHEMICALS Inc., USA), used to obtain the polymeric coating based on acetate cellulose (coded CA) and composite coatings based on cellulose acetate reinforced with hydroxyapatite (HAp) and magnesium (Mg) particles (coded CAHAp, CAMg, CAHApMg).
- ➢ Magnesium alloys, Mg3Nd_A and Mg3Nd_B, coated with a composite layer based on cellulose acetate (coded Mg3Nd_A CAHAp and Mg3Nd_ A_ CAMg, Mg3Nd_ B_ CAHAp and Mg3Nd_B_CAMg). In order to characterize, test and demonstrate the functionality of coated Mg3Nd alloys, samples of Mg3Nd alloys with dimensions of 15×15×5 mm were used$_3$ (width×length×height) covered.

The work plan

- ➢ Selection, based on biofunctionality criteria, of magnesium alloys potentially usable as orthopedic biomaterials (**two biodegradable magnesium alloys from the Mg3Nd system with different Y content, respectively Mg3Nd_A and Mg3Nd_B**);
- ➢ Selection of the optimal surface modification method of experimental Mg3Nd alloys (**composite polymer coatings based on cellulose acetate, using the immersion method**);
- ➢ Microstructural characterization of two experimental Mg3Nd alloys, respectively Mg3Nd_A and Mg3Nd_B, by: MO, SEM-EDS, XRD;
- ➢ Deposition of composite polymer coatings, using the immersion method, on the surface of the experimental magnesium alloys Mg3Nd_A and Mg3Nd_B;
- ➢ Characterization of composite polymer coatings by: SEM-EDS, FTIR, RAMAN;
- ➢ Determination of the surface properties of composite polymer coatings by the contact angle method;
- ➢ Thermogravimetric analysis of composite polymer coatings;
- ➢ Functional testing of composite polymer coatings, in PBS solution, by determining mass loss and swelling rate;
- ➢ Functional testing of composite polymer coatings by performing biocompatibility tests*in vitro*, following cellular cytotoxicity (MTT test and cell viability test with Calcein AM);
- ➢ Characterization of coated Md3Nd alloys by SEM-EDS;
- ➢ Determination of the surface properties of coated and uncoated Mg3Nd alloys by the contact angle method and profilometry;
- ➢ Functional testing of coated and uncoated Mg3Nd alloys, in simulated physiological fluid solution - SBF, by: determination of the amount of hydrogen released, determination of pH, determination of mass loss;
- ➢ Functional testing of coated and uncoated Mg3Nd alloys, in simulated physiological fluid solution - SBF, by performing electrochemical corrosion tests;
- ➢ Functional testing of coated and uncoated Mg3Nd alloys by performing biocompatibility tests*in vivo*on laboratory rats, Whistar breed.

CHAPTER 4. STRUCTURAL CHARACTERIZATION OF MAGNESIUM ALLOYS Mg3Nd

The composition of the experimental Mg3Nd alloys selected to be characterized and tested in order to evaluate their potential as raw materials in the manufacture of orthopedic implants for trauma is presented in Table 4.1.

Table 4.1. Chemical composition of Mg3Nd alloys

alloys	**Composition (wt. %)**				
	Zn	Zr	Y	when	Mgr
Mg3Nd_A	0.3	0.6	2.10	3.2	Prom.
Mg3Nd_B	0.3	0.4	0.21	3.1	Prom.

Zinc (Zn) is the second most abundant transition metal in the human body and is an essential element for biological functions such as nucleic acid metabolism, regulation of apoptosis, modulation of brain excitability, regulation of the endocrine system [4]. The limited addition of Zn (up to 4 wt.%) in Mg-based alloys can cause a reduction in the corrosion rate [5]. However, the maximum solubility for Zn in Mg is 6.2 wt.% at the eutectic temperature, and becomes lower at room temperature. As the zinc content increases (over 4

wt.%) corrosion resistance decreases due to increased precipitation phases at grain boundaries and increased galvanic effect [6].

The main role of zirconium (Zr) is to refine the microstructure of magnesium alloys [7,8]. Its influence on the corrosion rate depends primarily on its concentration and distribution in the alloy structure. A high content of Zr in solid solutions (~0.5 wt.%) can activate anodic reactions, thus accelerating the overall corrosion of the magnesium alloy matrix and increasing the long-term corrosion rate [9-12]. However, in several ternary (and higher order) alloys, the addition of Zr has been shown to stabilize the magnesium solid solution, inactivating the material during anodic dissolution and reducing cathodic hydrogen evolution [13,7,14].

Rare earths (RE) contribute to the improvement of mechanical properties, having an important influence on the alloy texture and corrosion behavior. In [16,17] it was observed that the addition of rare earths improves the performance of alloys at high temperature. The most commonly used rare earths as alloying elements with Mg are cerium (Ce), neodymium (Nd), yttrium (Y), gadolinium (Gd), lanthanum (La) and praseodymium (Pr). Rare earths form a Mg-Zn-RE ternary eutectic compound, which improves the creep strength and casting of Mg-Zn-Zr alloys [18]. Loss et al [19] investigated the biocompatibility of yttrium based on tests *in vitro* and *in vivo* performed on samples from Mg stents. It has been observed that when a high concentration of Y is used it can accumulate in the bile and in the liver. Also Y can increase the level of eosinophils in the blood having a negative effect on the biocompatibility of the implant. Other studies have shown that Nd addition needs to be done only within certain limits to control the formation of the Mg binary phase Mg_3Nd in Mg-Nd alloys, because otherwise this phase causes an increase in the corrosion rate.

4.1. Optical microscopy determinations

In the preparation of the samples from the Mg3Nd_A and Mg3Nd_B alloys, for the microstructural evaluation, the following stages are performed: Stage I - Cutting the samples; Stage II - Embedding; Stage III - Grinding / Polishing; Stage IV - Metallographic attack.

Figures 4.3 and 4.7. shows the optical microscopy images, at different magnifications, corresponding to Mg3Nd_A and Mg3Nd_B alloys before and after the metallographic attack.

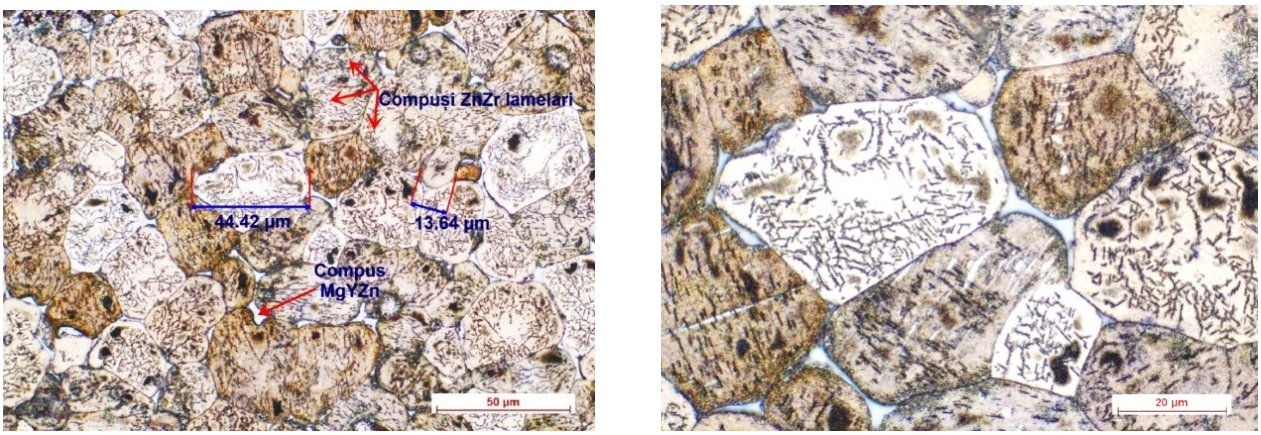

Figure 4.3. Optical microscopy images for Mg3Nd_A alloy (10×, 50×) after chemical attack

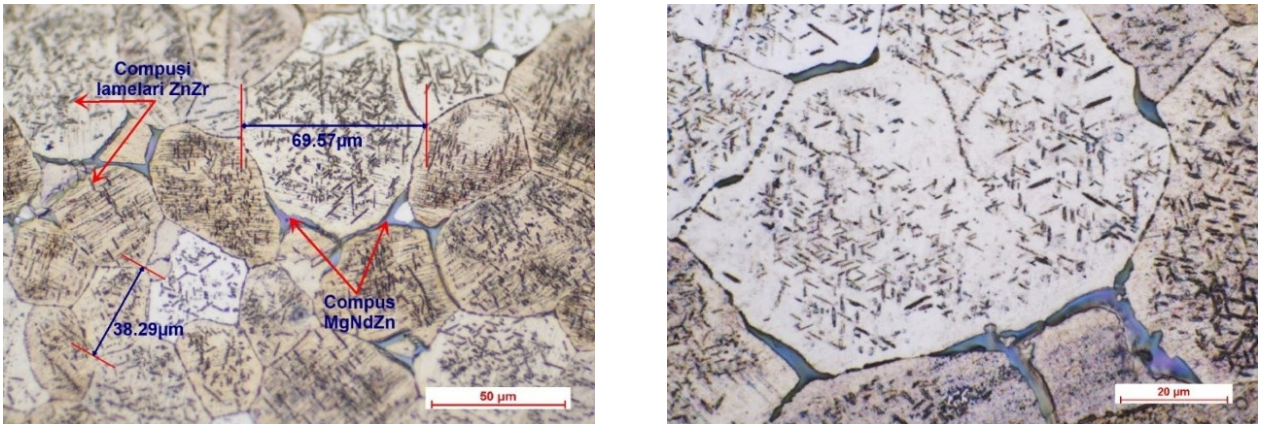

Figure 4.7. Optical microscopy images for Mg3Nd_B alloy (10×, 50×) after chemical attack

The microstructure of the alloys consists of fine and uniform polyhedral α-Mg grains, in which secondary phases are precipitated, with different morphologies, from acicular to globular, uniformly distributed inside the α-Mg grains.

Micrographs also reveal a distinct grain boundary phase, most likely a multicomponent intermetallic compound.

In the Mg3Nd_A alloy, compared to the Mg3Nd_B alloy, the grains are smaller and more uniform in size, the degree of intragranular precipitation is higher, and acicular (icosahedral) compounds are the majority, tending to group "in bundles" which will increase considerably the mechanical properties of the alloys.

The effect of the presence of a larger amount of Y in the chemical composition of the Mg3Nd_A alloy is realized by the refinement of the microstructure of the alloy, a decrease in the size of the grains and their uniformity.

Also, the proportion of the phase at the grain boundaries is visibly reduced in the Mg3Nd_B alloy, becoming insular, which will increase the ductility of the alloy.

4.2. Scanning Electron Microscopy (SEM) Determinations Coupled with Energy Dispersive X-ray Spectroscopy (EDS)

Figures 4.9 and 4.10. highlights SEM images and EDS analysis on Mg3Nd_A and Mg3Nd_B alloys, at different magnifications.

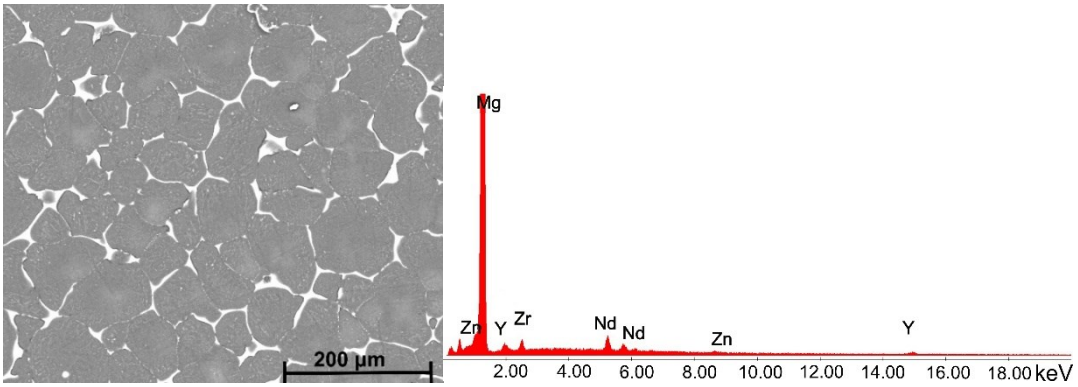

Figure 4.9.SEM image and EDS spectrum for Mg3Nd_A alloy

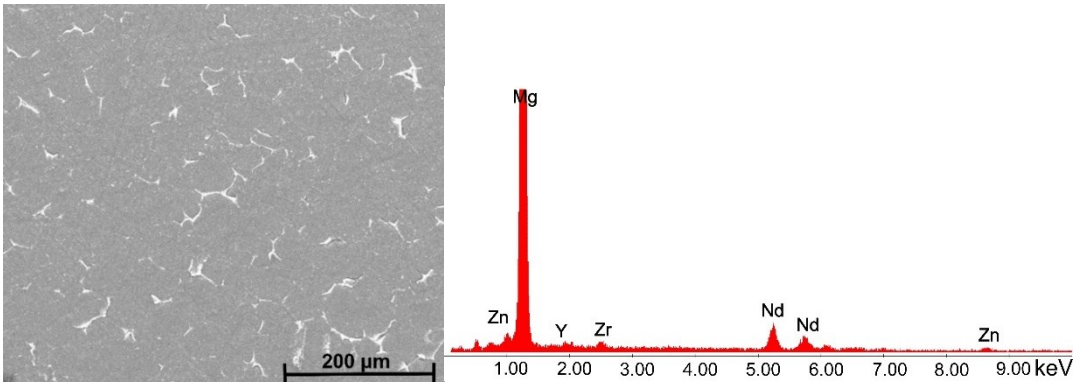

Figure 4.10.SEM image and EDS spectrum for Mg3Nd_B alloy

The results support the optical microscopy investigation, highlighting the morphology and distribution of the secondary phases.

According to the EDS results for the Mg3Nd_B alloy, the phase identified at the grain boundary was found to be rich in Mg, Zn and Nd. By increasing the amount of Y in the composition of the alloy (Mg3Nd_A alloy), the formation of a grain boundary rich in Mg, Zn, Nd and Y is observed. Elkaimey et al. [63] and Zengin et al [62] proposed that the phase be identified as $Mg_3(Nd, Y)_2Zn_3$. Moreover, the granular compounds present in the alloy structure contain rare earths (Y and Nd), while the acicular compounds consist of Zr and Zn.

4.3. X-ray diffraction determinations

In Figure 4.15. XRD diffraction patterns of Mg3Nd_A and Mg3Nd_B alloys obtained by gravity casting are shown. As can be seen in the figure, the Mg3Nd_B alloy (0.21 wt.% Y) shows diffraction maxima corresponding to the α-Mg phase, the Mg-Zn-Nd ternary phase and the Mg-Zn-Y ternary phase. Yang et al. [16] also observed the presence of Mg-Zn-Nd phase in Mg4.5ZnxNd alloys with similar morphology and composition to Mg-Zn-Nd phase in Mg3Nd_B alloy and identified them as Mg phases$_4Zn_2Nd$ (T phase). Thus, it can be deduced that the Mg-Zn-Nd ternary phases in the Mg3Nd_B alloy correspond to the T phase with the chemical formula of Mg_4Zn_2Nd.

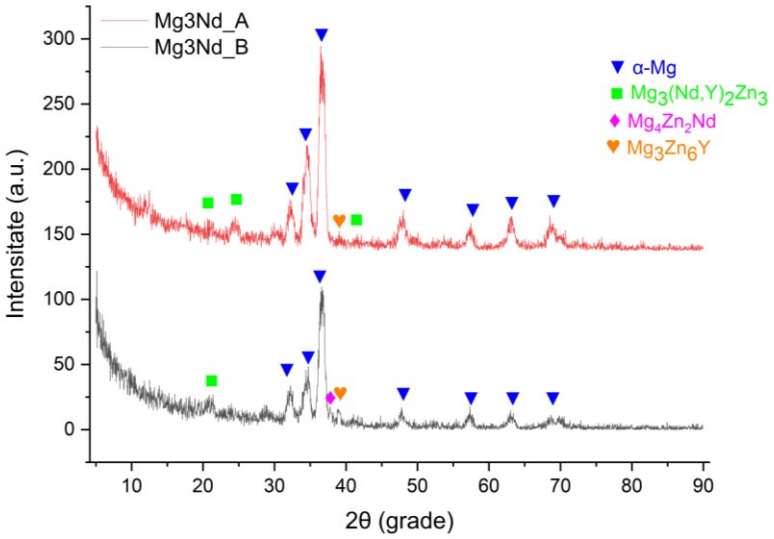

Figure 4.15.XRD diffractogram for Mg3Nd_A and Mg3Nd_B alloys

By increasing the amount of Y (Mg3Nd_A alloy) it is observed that the secondary phases contain more Mg, Zn and Y, but less Nd compared to the Mg3Nd_B alloy.

Thus, in the Mg3Nd_A alloy, the presence of the corresponding diffraction maxima is observed phase α-Mg, Mg_3Zn_6Y and $Mg_3(Nd,Y)_2Zn_3$. By increasing the Y content, the intensities of the diffraction maxima for the Mg phase$_3$(Nd,Y)$_2$Zn$_3$they grew up.

CHAPTER 5. OBTAINING AND CHARACTERIZATION OF COATINGS BASED ON CELLULOSE ACETATE

5.1. Obtaining coatings based on cellulose acetate

Cellulose acetate (CA) coatings and CA-based composite coatings reinforced with hydroxyapatite or magnesium particles have been synthesized with the aim of reducing the initial corrosion process of magnesium Mg3Nd alloys. Cellulose acetate is an important ester from the cellulose family having the advantages of being biocompatible, bioresorbable and also widely available and cheaper than other potential polymers used for metal implant coating such as polylactic acid or polycaprolactone.

The cellulose acetate and composite coatings were obtained by the solvent evaporation method.

The coding of the experimental samples is presented in table 5.1.

Table 5.1. Coding of experimental samples

Trial Code	Composition
THAT	cellulose acetate
CAHAp	cellulose acetate + 5% hydroxyapatite
CAMg	cellulose acetate + 5% Mg particles
CAHApMg	cellulose acetate+5% hydroxyapatite + 5% Mg particles

The appearance of CA coatings and composite coatings based on CA with hydroxyapatite and magnesium particles, after being kept in the oven, is presented in Figure 5.2.

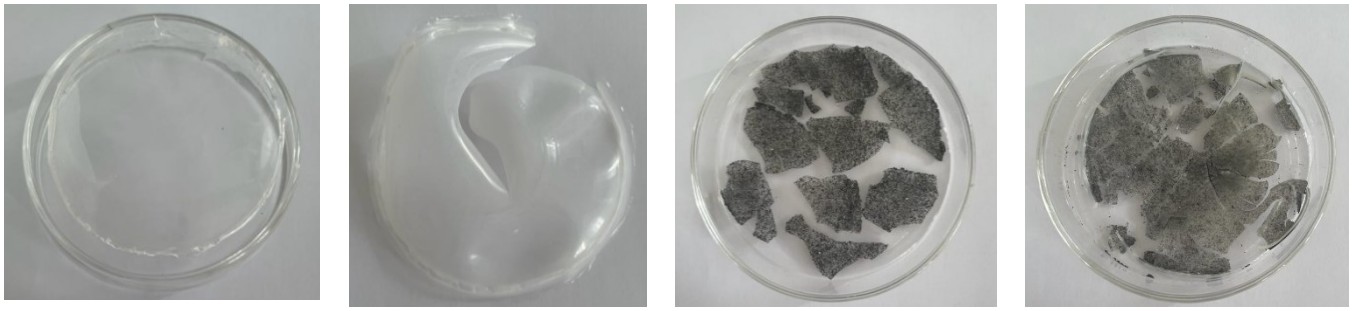

Figure 5.2. Appearance of obtained coatings

5.3. Morphological and structural characterization of cellulose acetate-based coatings

5.3.1. Characterization of coatings by scanning electron microscopy (SEM) coupled with energy dispersive X-ray spectroscopy (EDS)

The morphological characteristics of the obtained coatings were analyzed by scanning electron microscopy in order to investigate the general aspects of the surface, as can be seen in Figure 5.7.

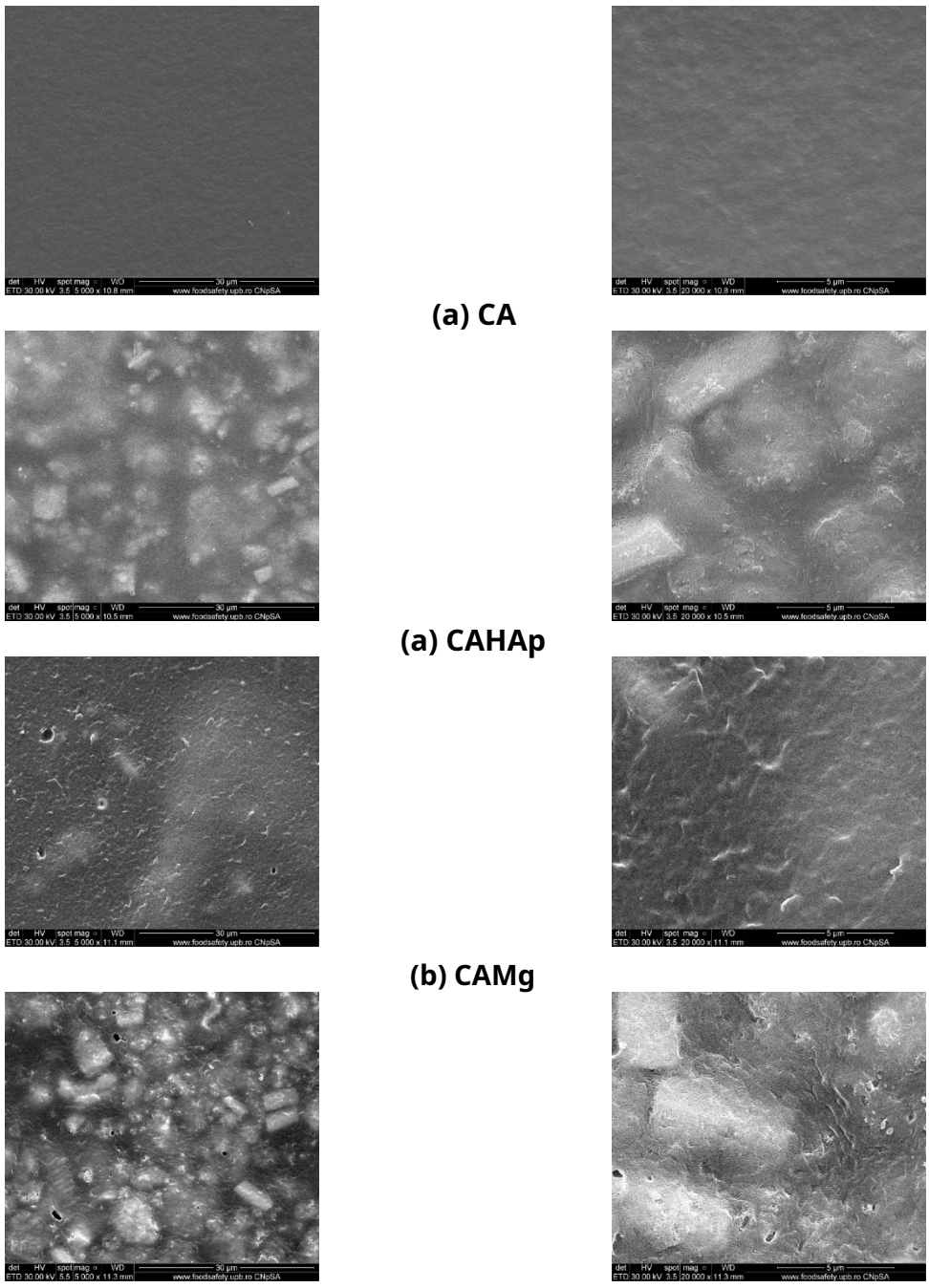

Figure 5.7. Characterization of the coatings: (a) CA, (b) CAHAp, (c) CAMg, (d) CAHApMg

In the SEM images taken on the polymer coating in CA, it is observed that after the evaporation of the solvent, a compact and homogeneous polymer film is obtained, a smooth surface. By adding magnesium particles to the polymer solution (CAMg, CAHApMg samples), we can observe the appearance of pores on the surface of the investigated samples. Furthermore, the SEM images show that the pores have irregular sizes and are unevenly distributed. Porosity exists due to the action of solvent molecules on the polymer film during the evaporation process, which leads to the formation of channels. Magnesium particles disperse more uniformly throughout the polymer mass (CAMg sample) than hydroxyapatite particles (CAHAp sample). Hydroxyapatite particles occur both in dispersed form and in the form of agglomerates (large crystals).

The elemental composition of the CA coatings and composite coatings was determined by Energy Dispersive X-ray Spectroscopy (EDS). EDS analysis confirms the presence and distribution of hydroxyapatite and magnesium particles in the structure of the composite coatings. Unlike the cellulose acetate sample in whose EDS spectrum (Figure 5.8.) only carbon (C) and oxygen (O) elements from the polymer structure were identified, in the case of composite coatings (Figure 5.9.), the presence of calcium was also identified (Ca) and phosphorus (P) from hydroxyapatite and magnesium (Mg) from magnesium particles.

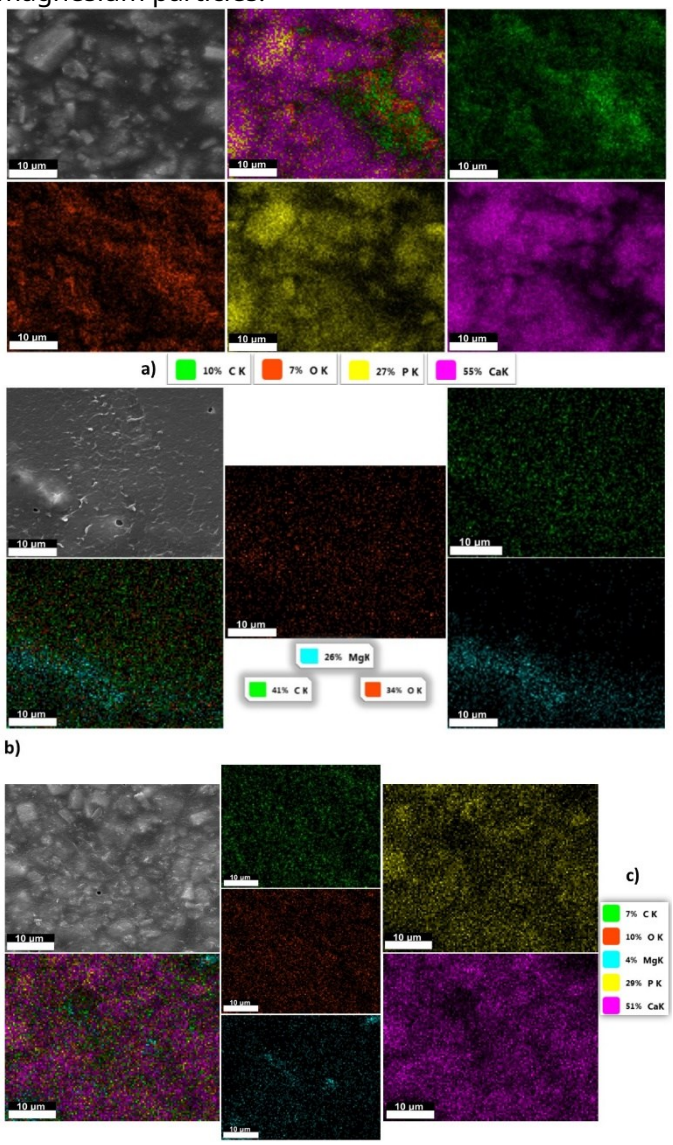

Figure 5.9.SEM images and EDS mapping for: (a) CAHAp, (b) CAMg, (c) CAHApMg

Thus, it was revealed that magnesium particles disperse more evenly throughout the mass of the polymer (CAMg sample) compared to hydroxyapatite particles (CAHAp sample). Hydroxyapatite particles occur both in dispersed form and in the form of agglomerates (large crystals).

5.3.2. Characterization of coatings by FTIR Spectroscopy

Fourier transform infrared spectroscopy (FTIR) was used to identify the specific functional groups or chemical bonds present in the investigated experimental samples (Figure 5.10.), revealing slight differences between the spectrum of the cellulose acetate (CA) coating and the spectra of the composite coatings. The spectra highlight the presence of characteristic bands for

cellulose acetate at ~1745 cm^{-1}($\nu_{C=O}$) attributed to the stretching vibration of the ester carbonyl (C=O) from the acetyl group, at ~1230 cm^{-1}($\nu_{Co.}$) attributed to the stretching vibration of the CO bond in the acetyl group and at ~1370 $cm^{-1}$and ~1430 cm^{-1}(δ_{CH}) bands due to the bending vibration of the CH bond in the -CH groups$_3$(acetyl group) and -CH_2(the pyranose ring).

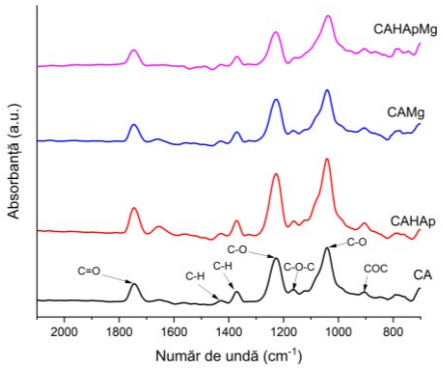

Figure 5.10.FTIR spectra for the investigated polymer coatings

The spectra of the composite coatings (CAMg, CAHAp, CAHApMg samples) are almost similar to the spectrum of the cellulose acetate coating. The band corresponding to the vibration of the CO bond at 1040 cm^{-1}shifted to the right in the case of CAHAp and CAHApMg composite coatings due to the influence of PO groups[34]from hydroxyapatite occurring in the same region of the spectrum.

In the FTIR spectra of the composite coatings, there are no two distinct bands for CO and PO bond vibrations due to the small content of inorganic particles contained and the overlapping of the vibration bands characteristic of hydroxyapatite in the range of 600-1100 $cm^{-1}$with the appropriate polymer strips.

5.3.3. Characterization of coatings by RAMAN Spectroscopy

From Figure 5.11. it is observed that the CA coating and the CAMg composite coating have similar morphologies. This indicates that the Mg particles are uniformly distributed in the coating, in direct correlation with the aspects highlighted by scanning electron microscopy.

In contrast, the addition of HAp particles leads to segregated areas, showing a high degree of agglomeration. This fact may be related to the crystallization and segregation of HAp particles from the solution. And the CAHApMg sample shows some degree of segregation, although the chemistry may be different due to the presence of Mg particles.

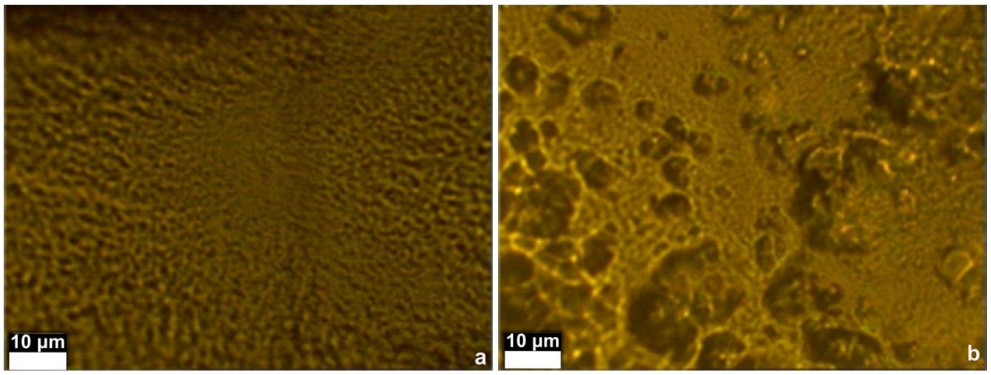

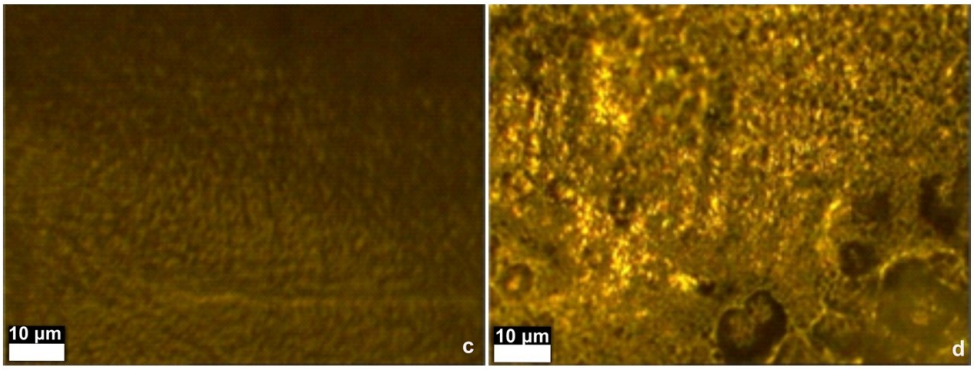

Figure 5.11. Images (50X) obtained for (a) CA sample, (b) CAHAp sample, (c) sample of CAMg and (d) CAHApMg sample

The Raman spectrum of hydroxyapatite (HAp) shows the main features assocd PO_4 groupings and OH^- [6]. PO_4 grouping is characterized by the band due to the vibration of symmetric elongation (P–O) from 973 cm^{-1}, the band due to the bending vibration (O–P–O) from 430– 450 cm^{-1}, the band due to the asymmetric stretching vibration (P–O) from 1020–1080 cm^{-1} and the band due to the bending vibration (O–P–O) from 585–610 cm^{-1}. The presence of the OH group causes the appearance of bands due to the stretching vibration from 3600 cm^{-1}, of the vibrational band from 630 cm^{-1} and of the translation band from 340 cm^{-1}.

In Figure 5.11.a, the Raman spectrum of the CA coatings is associated with the vibrational bands at 2945 cm^{-1} and 1129 cm^{-1} [7]. They are attributed to the stretching vibration of the CH bond and the asymmetric stretching vibration of the COC glycosidic bond. Additionally, the contribution of the pyranose ring is seen at 1081 cm^{-1}. The vibrational band associated with C-OH bonds is observed at 1272 cm^{-1}. Characteristic Raman signals for the acetyl group can be observed at 1744, 1443 and 1390 cm^{-1}, corresponding to the vibrations of the carbonyl group (C=O) and the asymmetric and symmetric vibrations of the CH bond. Vibrational bands at 986, 914, 842, and 667 cm^{-1} are associated with CO, CH, OH and C-OH bonds, respectively.

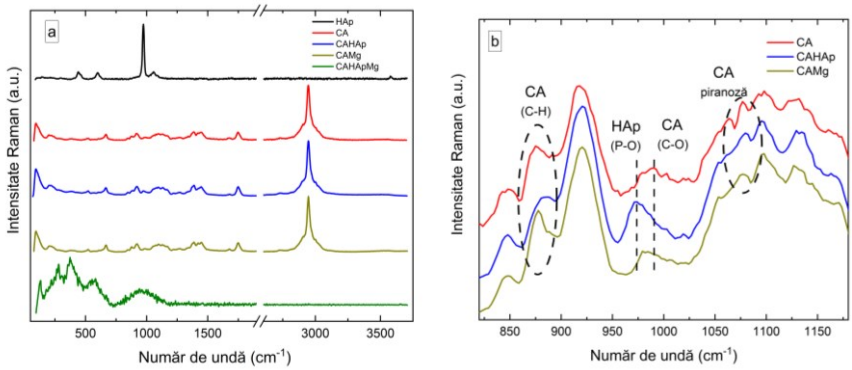

Figure 5.12. Raman spectra of (a) HAp, CA coating and composite coatings; (b) CA, CAHAp, CAMg in the range 800-1200 cm^{-1}

5.3.4. Thermogravimetric analysis

Thermogravimetric analysis (TGA) was used to study the effect of hydroxyapatite and magnesium particles on the thermostability of the polymer. Figure 5.13. illustrates the TGA curves of the cellulose acetate (CA) coating and the composite coatings (CAHAp, CAMg, CAHApMg). According to the figure, all samples show a similar profile with two degradation stages. The first stage of degradation corresponds to the evaporation of traces of solvent (between 150 °C and 230 °C) from

polymer coatings, and the second is due to the decomposition of the polymer chain (from 250 °C to 370 °C).

The lowest thermostability is shown by cellulose acetate coating, thermal resistance increasing with the addition of filler particles. This was tested by measuring the decomposition temperature after losing 10% of the mass of the investigated samples (T_d10%). T values$_d$10% are: 265.71 °C for CA coating; 319.59 °C for CAHAp coating; 317.10 °C for the CAMg coating and 313.3 °C for the CAHApMg coating.

The CAHApMg sample containing both types of particles (hydroxyapatite and magnesium) has an intermediate behavior, the thermostability being given by a competition between the two mechanisms.

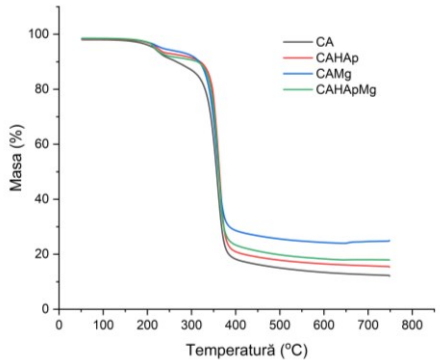

Figure 5.13.TGA curves for experimental coatings (CA, CAHAp, CAMg and CAHApMg)

5.4. Functional characterization of cellulose acetate based coatings

5.4.1. Determination of mass loss and swelling rate

The swelling rate of the investigated coatings for a period of up to 72 hours is presented in Figure 5.14. It can be seen from the figure that in the first 45 minutes, the swelling rate increases rapidly for all investigated coatings, but is more pronounced for those containing magnesium particles (CAMg and CAHApMg). The samples reach a steady state after 90 minutes, with a swelling of about 48% for the CAMg sample, 38% for the CAHApMg sample, and 32% for the CAHAp sample.

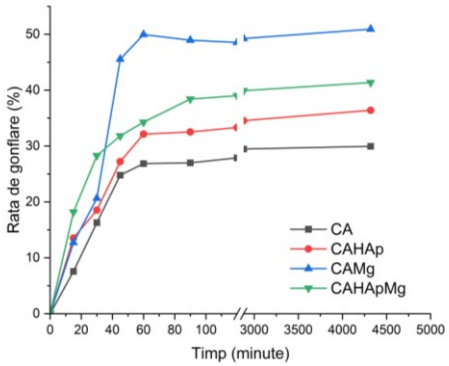

Figure 5.14. Swelling rate of coverslips over a period of 72 hours in PBS solution

The degradation behavior of the experimental coatings was evaluated by measuring the mass loss. The evolution of mass loss evaluated at 3, 7, 14, 21, 28 and 35 days of immersion in PBS is shown in Figure 5.15.

In the mass loss study, used to evaluate the degradation profile of the coatings, it was found that the degradation process occurred faster in the first 3 days of immersion for all the investigated coatings. In the following periods, coverage from CA and composite coverage with

CAHAp hydroxyapatite particles, show lower degradation rates, the increase from one interval to another being smaller and constant.

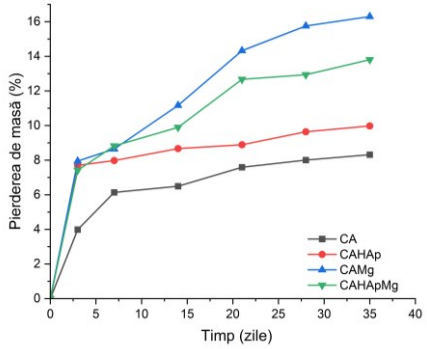

Figure 5.15. Degradation profile of the coatings over a period of 35 days of immersion in the solution by PBS

Wetting of the surface, quantified by measuring the value of the contact angle (Table 5.2.), represents an important factor in the functionality and biocompatibility of implantable devices [8,9]. The lowest values of the contact angle were obtained for the samples containing magnesium particles (CAHApMg and CAMg), which proves that by adding them, hydrophilic surfaces favorable for biological integration are obtained.

Table 5.2. Contact angle values

samples	Contact angle (degrees)
THAT	61.80±0.53
CAHAp	48.54±0.62
CAMg	42.05±0.49
CAHApMg	46.09±0.55

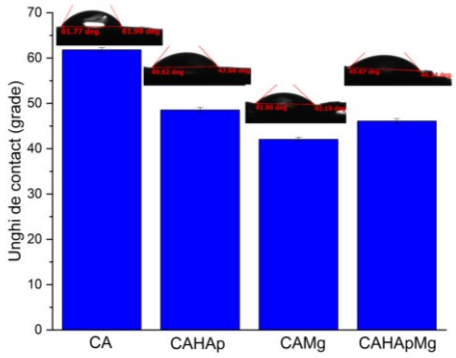

Figure 5.16. Contact angle values and water drop shape on the investigated coatings

5.4.2. In vitro biocompatibility testing by MTT assay and Calcein-AM cell viability assay

MTT assay

The results of the MTT assay are shown in Figure 5.17. Analyzing the results obtained on the tested inorganic particles, it is clear that the 100% extract is cytotoxic, the values obtained at 24 hours being 45.54% for HAp particles and 50.65% for Mg particles, while at 72 hours cell viability was found to be 56.58% for HAp particles and 55.86% for Mg particles. In the case of HAp particles, the cytotoxic behavior was also maintained for the 50% extract at 24 hours (54% viability), but an interesting phenomenon was observed at 72 hours, when cell viability increased significantly to 84.53%, suggesting a

mild initial toxic effect. Regarding Mg particles, it can be stated that this material is non-cytotoxic at a concentration of 50 % extract for both contact times.

For experimental CA-based coatings tested in direct contact with cells, the results are represented in Figure 5.18. For the CA polymer coating (from cellulose acetate) at 24 hours the cell viability was 63% and at 72 hours it increased to 75%

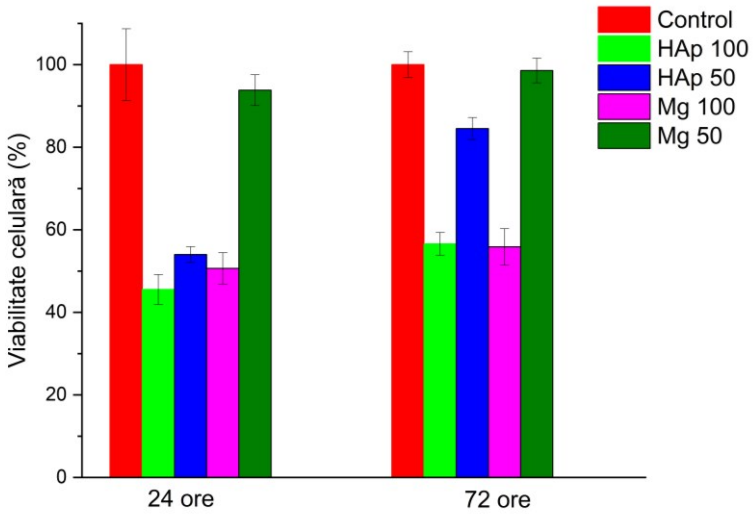

Figure 5.17. Cell viability, measured by the MTT assay, by indirect contact (extracts)

The introduction of both HAp and Mg particles into the CA solution decreases cell viability and more tests are needed in the future to establish the optimal ratio in which they must be combined so that the coating does not have a cytotoxic effect.

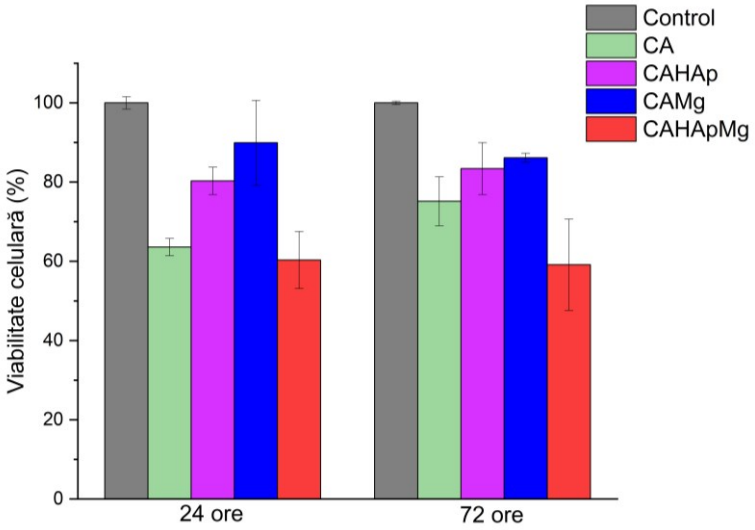

Figure 5.18. Cell viability as measured by direct contact MTT assay

Optical microscopy images of MG-63 cell line in direct contact (at 24 and at 72 hours) with the experimental coatings are shown in Figure 5.19. Images were captured with a fluorescence confocal microscope, Leica, Germany (10× objective).

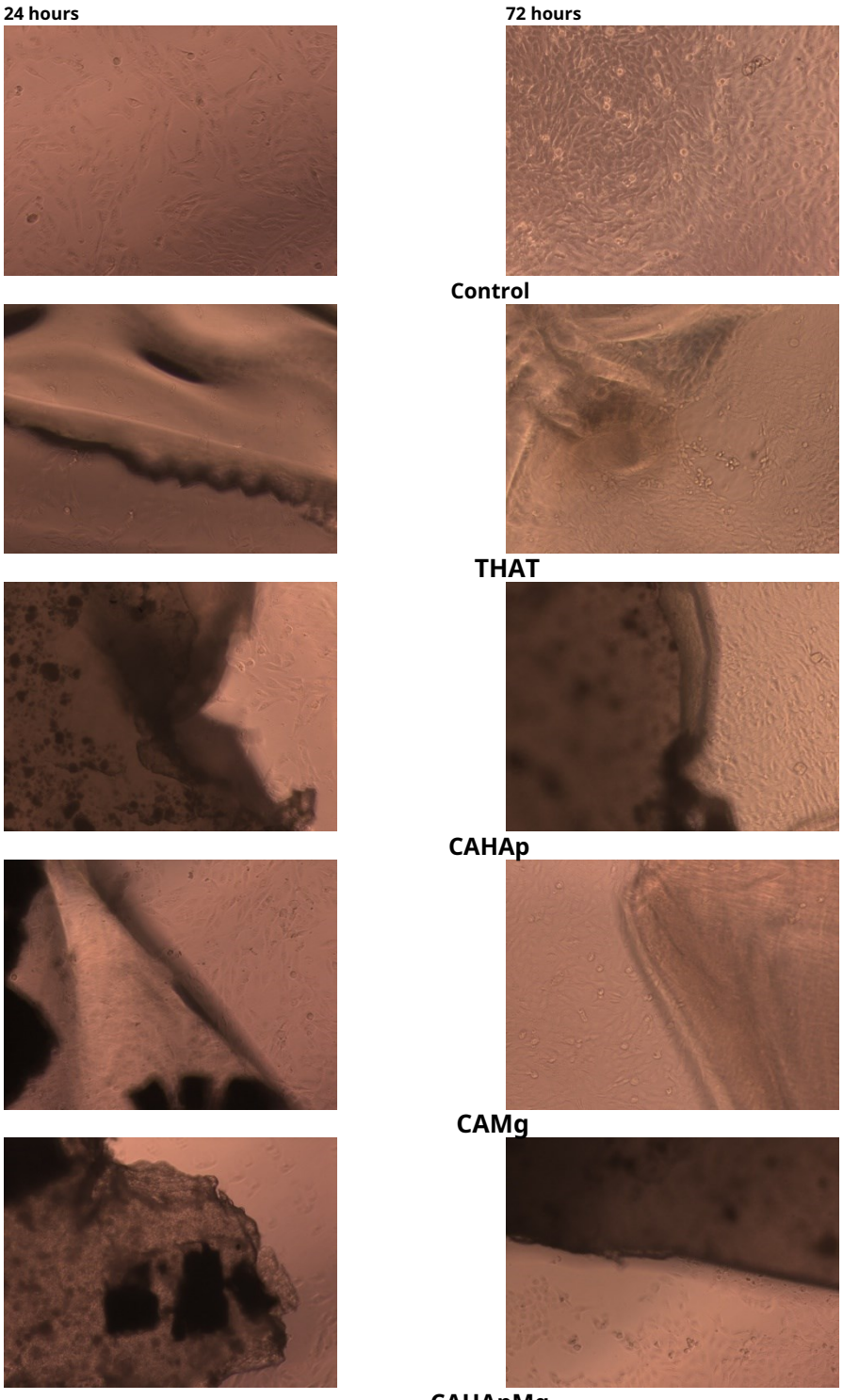

Figure 5.19. Optical microscopy images of MG-63 cell line in direct contact (24 and 72 of hours) with the experimental samples

Calcein AM Cell Viability Assay.

MTT assays revealed that the viability of cells incubated with CAHAp was 83% and with CAMg was 86% after 72 hours of direct contact; In both cases, the cell viability assay with Calcein-AM confirmed the values.

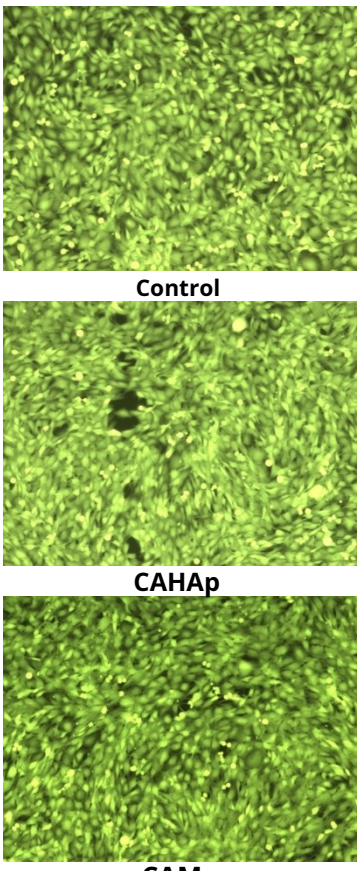

Figure 5.20. Fluorescence microscopy images of CAHAp and CAMg coatings in contact with cell cultures for 72 hours (Calcein AM dye). Images obtained with fluorescence confocal microscope, Leica, Germany (10× objective).

Analyzes performed on experimental composite coatings revealed the positive effect of magnesium and hydroxyapatite particles when used alone. It is not recommended to use both types of particles (hydroxyapatite and magnesium) as a hybrid filler.

CHAPTER 6. MODIFICATION OF THE SURFACE OF MAGNESIUM ALLOYS Mg3Nd BY MAKING COMPOSITE COATINGS BASED ON CELLULOSE ACETATE THROUGH THE DIP COATING METHOD

6.1. Experimental work protocol for obtaining coated Mg3Nd alloys

Following the study carried out on cellulose acetate (CA) coatings and polymer coatings based on cellulose acetate with hydroxyapatite and magnesium particles (CAHAp, CAMg, CAHApMg) two coatings were selected that correspond in terms of morpho properties -structural, surface and functional to be used in the coating of Mg3Nd magnesium alloys. These coatings are: CAHAp, CA-based composite coating with HAp particles and CAMg, CA-based composite coating with Mg particles.

The deposition of coatings on the surface of Mg3Nd alloys was achieved by immersing the alloy samples in the cellulose acetate solution with hydroxyapatite or magnesium particles. Through this method, uniform coatings with variable thicknesses are obtained due to the control of the process parameters and it allows the realization of layers on a multitude of materials with variable geometry

The polymer solution was obtained, under strong mechanical stirring, by dissolving cellulose acetate in N,N'-dimethylformamide. Hydroxyapatite (HAp) and magnesium (Mg) particles have

were dispersed, by ultrasonication for 30 minutes, in the polymer solution in a proportion of 5 wt.% relative to the amount of cellulose acetate. For the coating of Mg3Nd alloys, samples with dimensions of 15×15×5 mm^3(length × width × height) were immersed in the obtained polymer solution, extracted and kept for 3 days at a temperature of 45°C to evaporate the solvent. To obtain a homogeneous coverage, the operation was repeated three times.

After the coating process, the samples were coded as follows:

- ***Mg3Nd_A_CAHAp***–Mg3Nd_A alloy with CA-based composite coating reinforced with HAp;
- ***Mg3Nd_A_CAMg***-Mg3Nd_A alloy with Mg-reinforced CA-based composite coating;
- ***Mg3Nd_B_CAHAp***–Mg3Nd_B alloy with CA-based composite coating reinforced with HAp;
- ***Mg3Nd_B_CAMg***–Mg3Nd_B alloy with Mg-reinforced CA-based composite coating. Prior to characterization and testing, the experimental samples were washed with ethanol (Sigma-Aldrich, St. Louis, MO, USA).

The working protocol for obtaining coated Mg3Nd alloys is shown schematically in Figure 6.2.

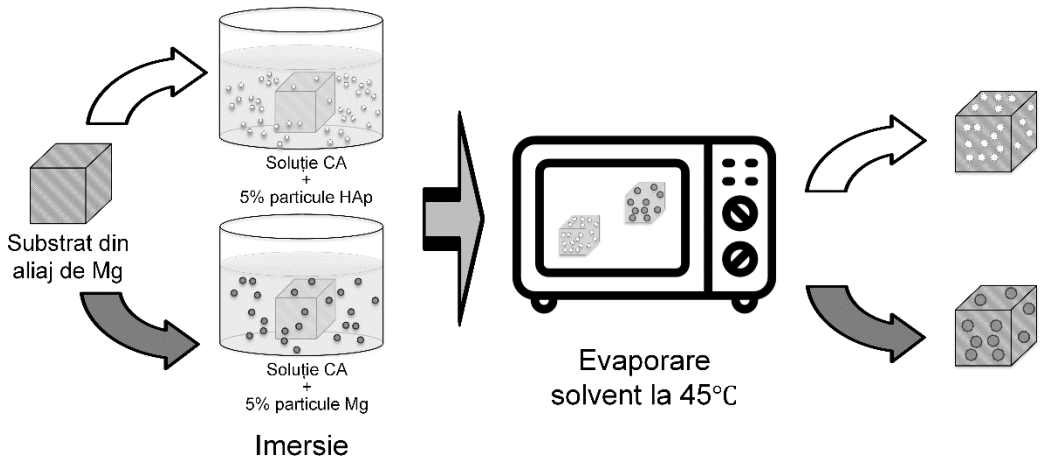

Figure 6.2. Schematic of the process of obtaining coated Mg3Nd magnesium alloy samples

6.2. Characterization of coated Mg3Nd alloys by scanning electron microscopy (SEM) The surface morphology of the coated Mg3Nd alloys and the layer thickness were revealed using scanning electron microscopy (SEM) Figure 6.3.

SEM images of HAp composite polymer coatings (Mg3Nd_A_CAHAp and Mg3Nd_B_CAHAp) on Mg3Nd alloys reveal a homogeneous distribution of particles in the polymer matrix. Through the evaporation of the solvent, very compact polymer composite coatings with small diameter pores were formed, giving a smooth character to the surface. The porosity exists due to the action of the solvent molecules, N,N'-dimethylformamide, on the composite coating during the evaporation process, which leads to the formation of channels. The main conclusion to be drawn is that the developed coatings are well made, the working parameters were well chosen with a much smoother surface in the case of the Mg particle composite coating.

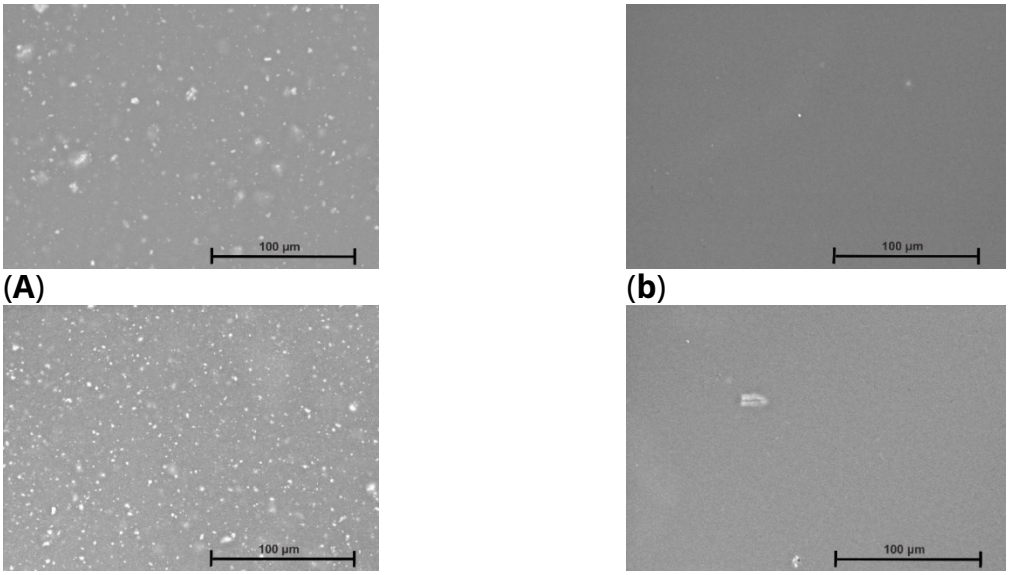

(**A**) (**b**)

(**c**) (**d**)

Figure 6.3.SEM images of coated Mg3Nd alloys: (a) Mg3Nd_A_CAHAp; (b) Mg3Nd_ A_ CAMg; (c) Mg3Nd_ B_ CAHAp; (d) Mg3Nd_ B_ CAMg

6.3. Determination of surface properties of coated and uncoated Mg3Nd alloys

6.3.1. wettability

Figure 6.5. shows the appearance of droplets on the surface of Mg3Nd_A and Mg3Nd_B alloys, in the case of using water as a wetting agent, for the control samples (uncoated samples, Mg3Nd_A and Mg3Nd_B) and coated samples. It can be seen that in the case of Mg3Nd_A and Mg3Nd_B alloys, the CA-based composite coatings with HAp or Mg particles transform the surface of the alloy into a more hydrophilic one with the lowest contact angle value (52.79°) obtained for the Mg3Nd_B_CAMg sample . The HAp particles included in the composite coating cause a hydrophilic behavior of the surface with a contact angle of about 57.21° (Mg3Nd_B_CAHAp) and 64.23° (Mg3Nd_A_CAHAp).

It can be concluded that the coating procedure in the case of both Mg3Nd alloys is direct related to a hydrophilization of the surface with a much more predominant effect, in the case of the Mg3Nd_B alloy.

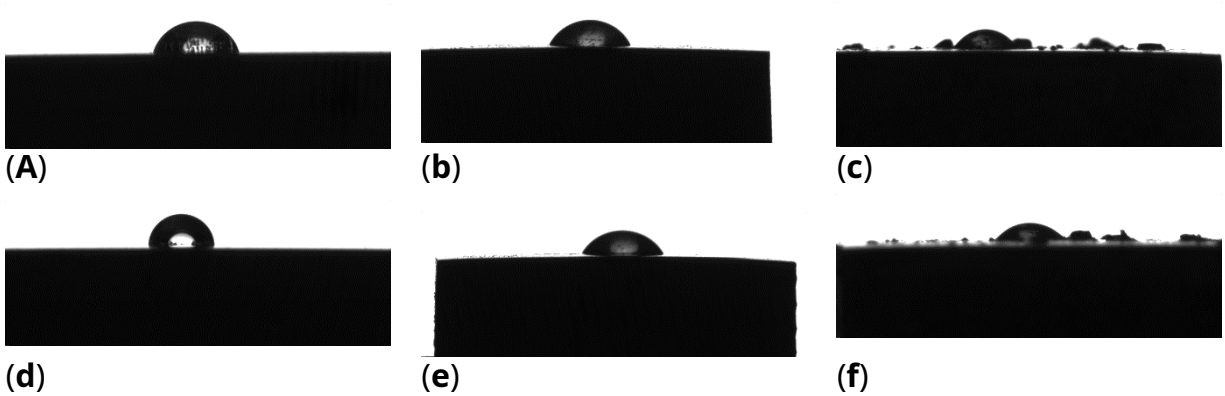

(**A**) (**b**) (**c**)

(**d**) (**e**) (**f**)

Figure 6.5. Drop shape and mean values obtained for experimental samples. For Mg3Nd_A: (a) control sample (70.37 ± 2.52°); (b) Mg3Nd_A_CAHAp (64.23 ± 1.19°); (c) Mg3Nd_A_CAMg (53.89 ± 1.98°); for Mg3Nd_B; (d) control sample (85.91 ± 2.02°); (e) Mg3Nd_B_CAHAp (57.21 ± 1.95°); (f) Mg3Nd_B_CAMg (52.79 ± 2.62°)

Based on the fact that ethylene glycol (EG) and water (W) are considered polar liquids, while diiodomethane (DIM) is a nonpolar/dispersive liquid, and their surface energy components are known as reported in [57], we calculated the surface free energy (SFE) of coated and uncoated alloys applying the OWKR method. The values obtained for the surface free energy are shown in Figure 6.7. In our case, the Mg3Nd alloy samples covered with the CA-based composite layer with HAp particles (Mg3Nd_A_CAHAp and Mg3Nd_B_CAHAp) presented the highest surface free energy values, and the lowest SFE value is specific to the Mg3Nd alloy samples uncovered.

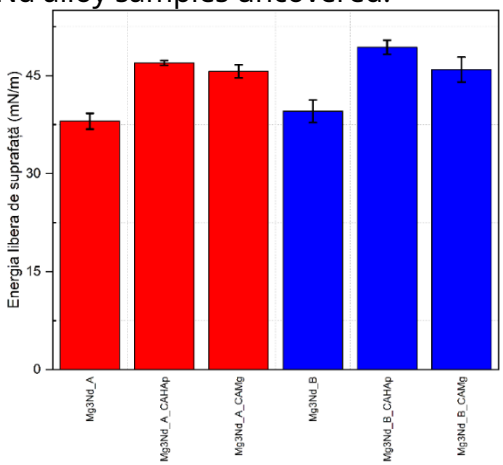

Figure 6.7. The surface free energy (SFE) values of the investigated samples, calculated with the OWKR method

6.3.2. roughness

The surface roughness for the samples developed in this PhD thesis (coated and uncoated Mg3Nd alloys) was investigated based on profilometric analysis. The roughness profiles and the determined parameter values are shown in the Figures below.

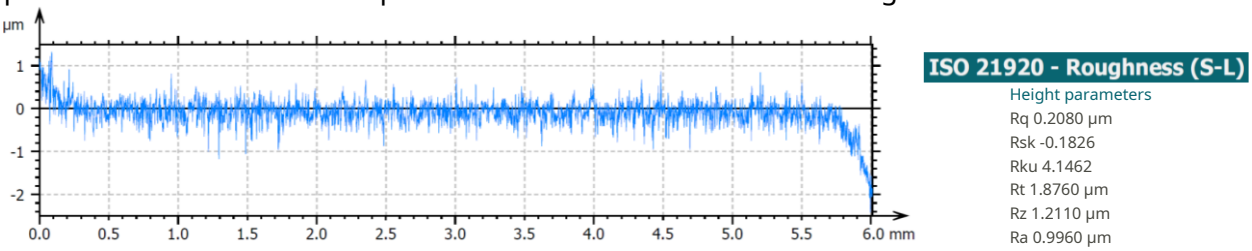

Figure 6.9. Roughness profile for sample Mg3Nd_A and determined parameters

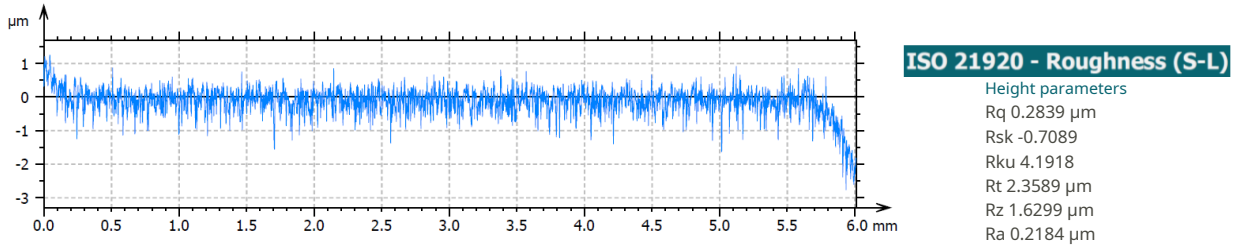

Figure 6.10. Roughness profile for sample Mg3Nd_B and determined parameters

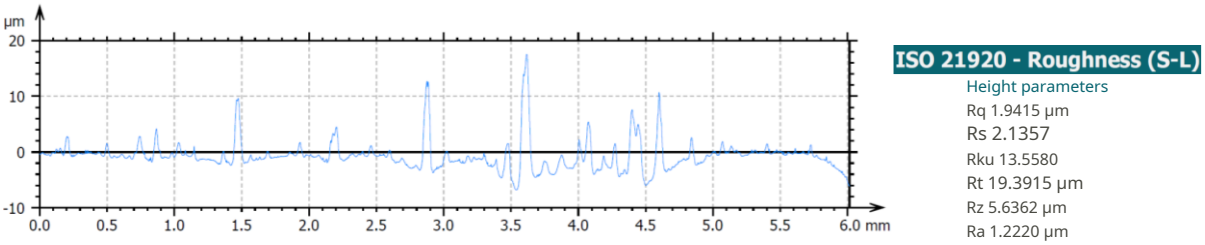

Figure 6.11. The roughness profile for the Mg3Nd sample_ A_ CAHAp and determined parameters

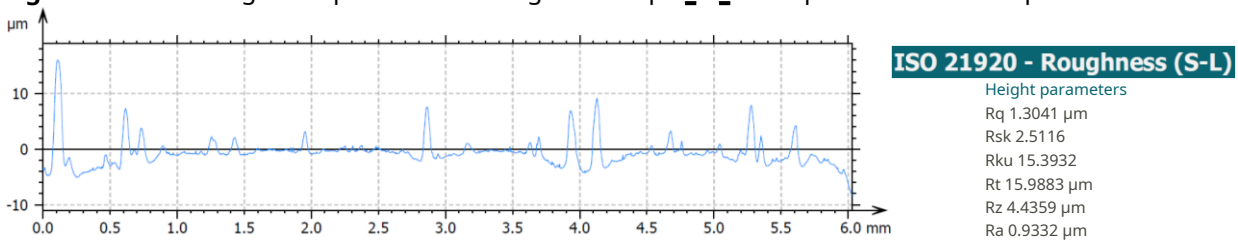

Figure 6.12. Roughness profile for Mg3Nd_B_CAHAp sample and determined parameters

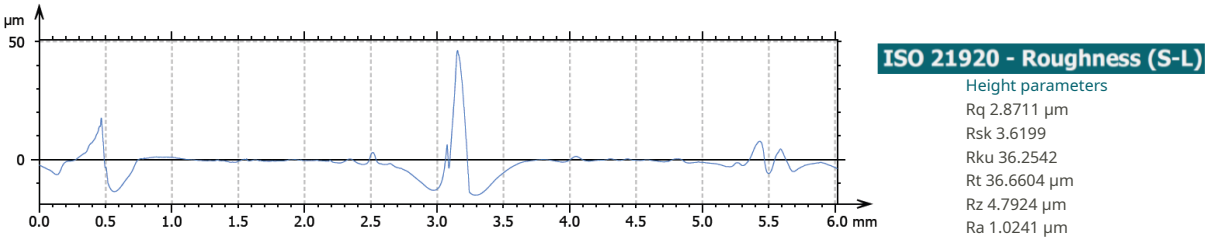

Figure 6.13. Roughness profile for Mg3Nd_A_CAMg sample and determined parameters

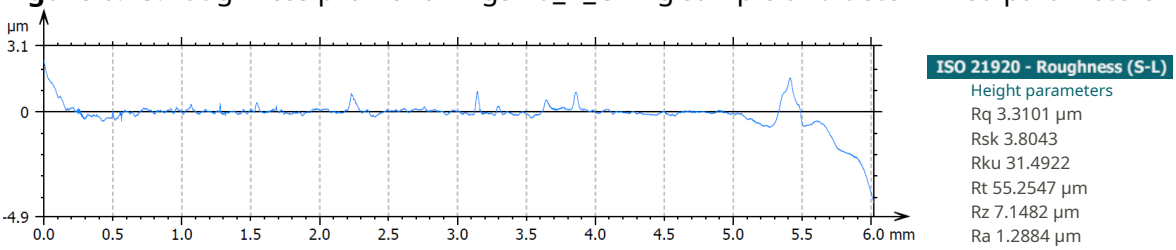

Figure 6.14. Roughness profile for Mg3Nd_B_CAMg sample and determined parameters

Our results showed that the uncoated Mg3Nd alloy samples had the lowest parameter values R_A and R_Q (Mg3Nd_A: R_A=0.996 ± 0.021 µm, R_Q=0.208 ± 0.023 µm; Mg3Nd_B: R_A=0.218 ± 0.022 µm, R_Q=0.284 ± 0.026 µm).

A correlation between the surface roughness and the degree of wetting was given in the literature by the Wenzel model [86]. This theory states that an increase in roughness will cause a decrease in the contact angle for hydrophilic surfaces. This correlation is valid in our case for both alloys. An increase in the surface roughness of the Mg3Nd alloys after coating was observed along with a decrease in the value of the contact angle (more hydrophilic surfaces were obtained), which will generate a better osseointegration of the implant made of these materials

6.4. Functional Testing of Coated and Uncoated Mg3Nd Magnesium Alloys

6.4.1. Determination of the corrosion behavior of experimental Mg3Nd magnesium alloys, before and after coating by immersion tests

Determination of mass loss

The evaluation of the corrosion behavior through the immersion test was carried out in the simulated physiological fluid solution at a temperature of 37 °C. The mass loss values obtained after 72, 168 and 336 hours of immersion are presented in Figure 6.16.

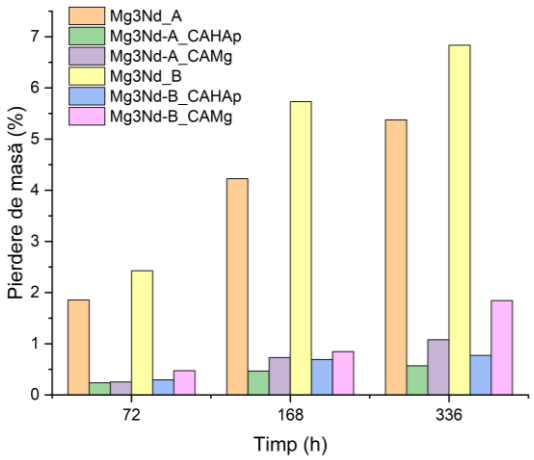

Figure 6.16. Evolution of mass loss of uncoated and coated Mg3Nd alloys in SBF solution

The lowest values were recorded for Mg alloys coated with cellulose acetate composite coatings with HAp particles (0.56% for Mg3Nd_A_CAHAp at 336 hours and 0.77% for Mg3Nd_B_CAHAp at 336 hours). For the uncoated alloys, the mass loss at 336 hours is 5.37% for the Mg3Nd_A alloy and 6.83% for the Mg3Nd_B alloy. The results highlight the beneficial effect of yttrium on the corrosion behavior of the alloys. A higher proportion of Y (2.10% in the Mg3Nd_A alloy compared to 0.21% in the Mg3Nd_B alloy) generates a lower mass loss and therefore a higher corrosion resistance due to the refinement of the alloy microstructure. Also, the results show that the composite coatings made on the surface of Mg3Nd alloys provide protection against the test environment. The results obtained for the Mg3Nd_A_CAHAp and Mg3Nd_B_CAHAp samples are respectively 10 and 9 times lower than the uncoated alloys, and for the Mg3Nd_A_CAMg and Mg3Nd_B_CAMg samples 5 and 4 times lower than the uncoated alloys, respectively.

Determination of the amount of hydrogen released

To estimate the corrosion rate of coated and uncoated Mg3Nd alloys, it was carried out the test to evaluate the amount of hydrogen released by the investigated samples using the simulated physiological fluid (SBF) solution as a test medium during 10 days. The hydrogen evolution experiments were carried out by also monitoring the pH evolution in the test medium.

The evolution of the hydrogen release rate and pH for the uncoated Mg3Nd_A and Mg3Nd_B alloys are shown in Figures 6.19. and 6.20.

From Figure 6.19. showing the evolution of the hydrogen release rate on the samples from uncoated alloys, a release rate of 2.4 ml/cm is observed after 24 hours of immersion$_2$for the Mg3Nd_A sample respectively of 2.9 ml/cm$_2$for the Mg3Nd_B sample, suggesting that the samples started to release hydrogen immediately after contact with the test solution (SBF), due to the low electrochemical potential of magnesium. The highest amount of hydrogen was released, in the case of both samples from Mg3Nd alloys, during the first 5 days of immersion, 8.9 ml/cm$_2$for the Mg3Nd_A sample with an alkalinization of the medium to a pH value of 8.55 and 10.1 ml/cm, respectively$_2$
for the Mg3Nd_B sample at a pH of 8.78. The obtained results indicate a higher corrosion resistance in the case of the Mg3Nd_A alloy, with a higher Y content, due to the refinement of its microstructure (smaller grain sizes).

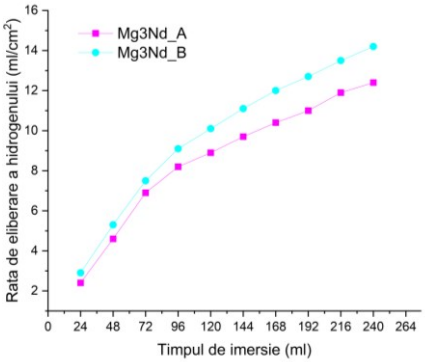

Figure 6.19. Hydrogen release rate, in SBF solution, for Mg3Nd_A and Mg3Nd_B alloys

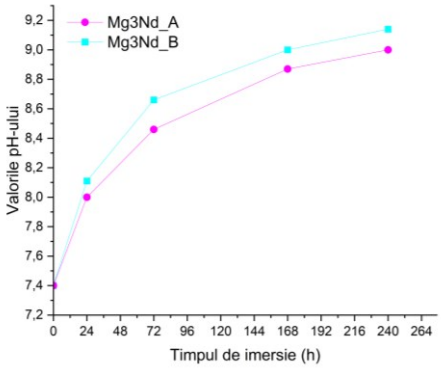

Figure 6.20. Variation of pH, in SBF solution, for Mg3Nd_A and Mg3Nd_B alloys

The evolution of hydrogen release rate and pH for Mg3Nd alloys are shown in Figures 6.21. and 6.22.

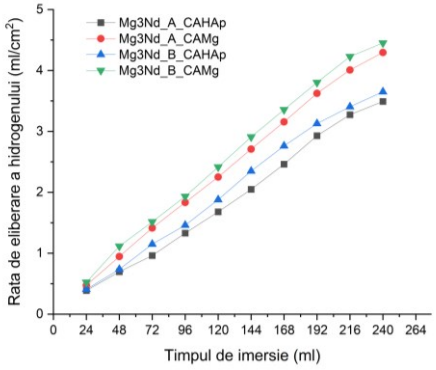

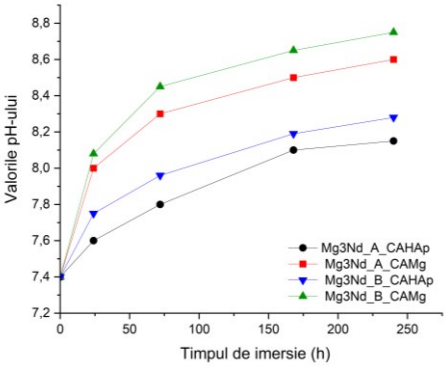

Figure 6.21. The hydrogen release rate,**Figure 6.22.**Variation of pH, in SBF solution, in SBF solution, for Mg3Nd alloys for Mg alloys$_3$Nd covered covered

For the samples from coated Mg3Nd alloys, the hydrogen release rate decreased considerably, registering, after 24 hours of immersion, values of 0.38 ml/cm for the coated Mg3Nd_A alloy$_2$(Mg3Nd_A alloy coated with CA-based layer and HAp particles, Mg3Nd_A_CAHAp) and 0.47 ml/cm$_2$(Mg3Nd_A alloy coated with CA-based layer and Mg particles, Mg3Nd_A_CAMg), and for the coated Mg3Nd_B alloy values of 0.40 ml/cm$_2$(Mg3Nd_B alloy coated with CA-based layer and HAp particles, Mg3Nd_B_CAHAp) and 0.52 ml/cm$_2$ (Mg3Nd_B alloy coated with CA-based layer and Mg particles, Mg3Nd_ B_ CAMg).

Regarding the pH evolution, a stronger alkalinization is observed in the samples from uncoated magnesium alloys compared to the coated ones. The presence of magnesium particles in the CAMg composite coating deposited on magnesium alloys (samples Mg3Nd_A_CAMg and Mg3Nd_B_CAMg) causes a stronger alkalinization of the test medium and higher hydrogen release rates compared to the composite coating with HAp particles. In Figure 6.23. hydrogen release rate values per day for coated and uncoated Mg3Nd magnesium alloys are presented.

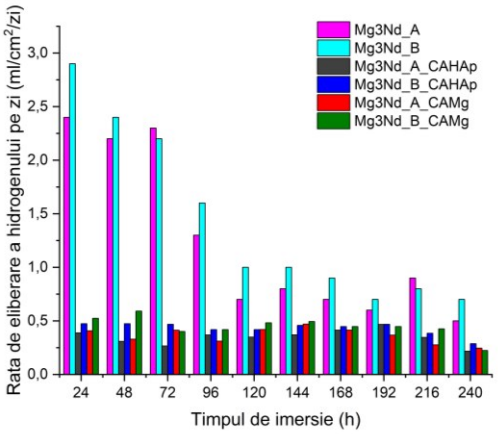

Figure 6.23. Hydrogen release rate per day, in SBF solution, for Mg3Nd alloys uncovered and covered

The values obtained for the uncovered alloys are, in the first 3 days of immersion, higher than the maximum values tolerated by the human body, after which they decrease in the following days, which makes it necessary to deposit a corrosion protection layer on their surface.

6.4.2. Determination of the corrosion behavior of experimental Mg3Nd magnesium alloys, before and after coating by electrochemical tests

The Tafel curves for coated and uncoated samples are shown in Figure 6.24.

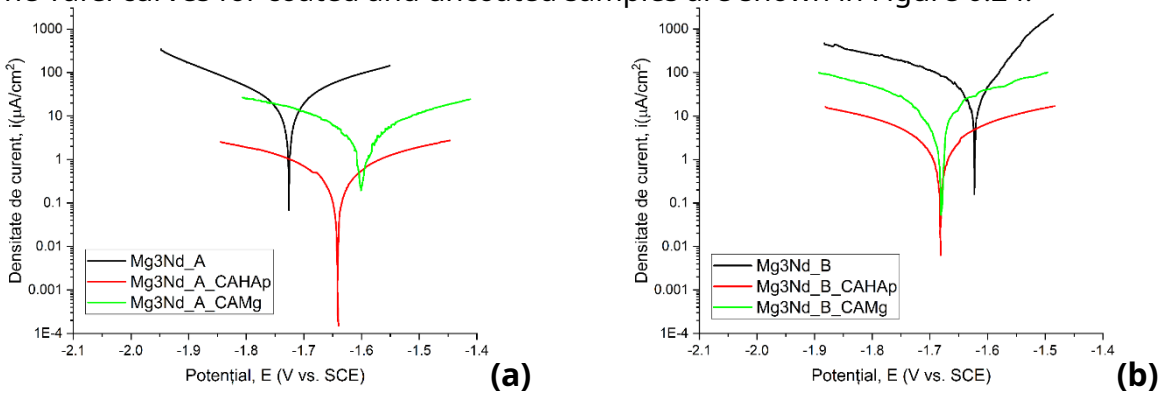

Figure 6.24. Tafel curves of uncoated and coated samples: (a) Mg3Nd_A; (b) Mg3Nd_B

The electrochemical parameters obtained for the uncoated and coated Mg3Nd alloys are shown in Table 6.1.

Table 6.1. Electrochemical test corrosion process parameters obtained on coated and uncoated Mg3Nd alloys

Sample code	E_{ok} (V)	E_{corr} (V)	i_{corr} (μA/cm²)	β_c (mV)	β_A (mV)	-R (mm/year)	p_e (%)	R_p (kΩcm²)
Mg3Nd_A	-1,765	-1,720	38,918	266.60	280,011	0.885	-	1,530
Mg3Nd_A_CAHAp	-1,647	-1,641	4,497	2637	1371	-	99.63	87,210
Mg3Nd_A_CAMg	-1,610	-1,605	16,684	625,154	676,912	-	98.66	8,469

Mg3Nd_B	-1,698	-1,699	55,689	268,870	87,419	1,266	-	0.535
Mg3Nd_B_CAHAp	-1,683	-1,681	14,971	1008	788,346	-	98.54	12,847
Mg3Nd_B_CAMg	-1,696	-1,678	20,607	297,275	242,764	-	97.99	2,819

The corrosion resistance of uncoated and coated Mg3Nd alloy samples was analyzed based on different evaluation criteria. It is well known that a more electropositive value of the open circuit potential (E_{ok}) is directly related to a more noble electrochemical character and a much better corrosion behavior in SBF. Analyzing the values presented in Table 6.1., it can be seen that all the coated samples showed better corrosion resistance than the uncoated alloys. The corrosion rate, calculated only for the uncoated Mg3Nd alloy samples, shows that Mg3Nd_A had a lower value (0.885 mm/year) than Mg3Nd_B (1.266 mm/year), so better corrosion resistance. The protection efficiency must have a higher value to indicate the protective effect of the coating against the corrosion phenomenon. This parameter can only be calculated for coated samples. For each type of Mg3Nd alloy, it can be seen that the best protection efficiency is provided by the composite coatings based on CA with HAp (Mg3Nd_A_CAHAp and Mg3Nd_B_CAHAp). As a final observation from the point of view of the protective effect of the coating, the best protective efficiency for both Mg3Nd alloys is provided by the composite coating based on *CA with HAp particles*. The two films developed resulted in increased corrosion resistance and have great potential to be used as coatings for magnesium alloy-based implants.

6.4.3. In vivo biocompatibility testing of coated and uncoated Mg3Nd magnesium alloys The clinical evaluation was performed immediately after the euthanasia of the laboratory animal. From the total of 24 laboratory animals, 2 specimens died immediately post-intervention, due to surgical and anesthetic trauma. No signs of systemic distress were observed for all other animals. In general, they did not identify signs of local inflammation, and when they did exist, they had a minimal or moderate intensity, being limited to the adjacent soft tissues, without being able to be correlated with a specific batch. Moreover, we noticed an individual variability both in terms of local inflammatory reactions and the speed of disintegration of the samples.

Figure 6.25. Clinical appearance of the internal face a ordeal in the case of a biological sample collected from a specimen from lot 1S Mg3Nd_A

Figure 6.27. Clinical appearance of the internal face of the calvaria in the case of a biological sample collected by to a specimen from batch 1S Mg3Nd_B

Figure 6.28. Appearance of the external face of the calvaria in the case of a biological sample collected from a specimen from batch 1S Mg3Nd_ A_ CAHAp

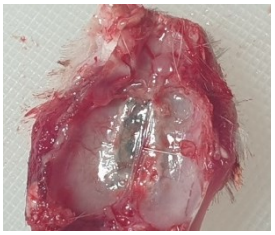

Figure 6.29. Clinical appearance of the internal face of the calvaria in the case of a biological sample collected by to a specimen from batch 1S Mg3Nd_ B_ CAHAp

Clinical microscopic evaluation .

The appearance of the sample from batch 1S Mg3Nd_A_CAHAp (Figure 6.35.) observed on the external face of the calvaria after detachment of the integument highlights the partial degradation of the sample and its replacement by fibrinous repair tissue. In Figure 6.37. which highlights a detail of a sample from batch 1S Mg3Nd_A_CAHAp observed on the external face of the calvaria, near a suture thread used to support the sample, it is covered by a loose connective tissue, but also the denser connective tissue, white in color, rich in fibers located at the periphery of the sample, which tends to replace it as it degrades.

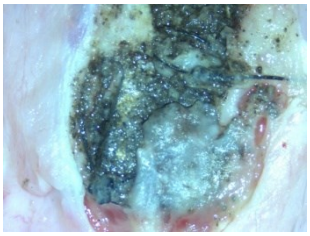

Figure 6.35. Appearance of the alloy sample from batch 1S Mg3Nd_A_CAHAp observed on the external face of Calvary after peeling off the skin (10x)

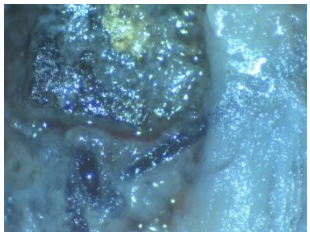

Figure 6.37. Detail of a batch 1S Mg3Nd_A_CAHAp alloy sample observed on the external face of the calvaria near a suture used for sample support (40x)

For the Mg3Nd_B alloy covered with CAHAp, the optical microscopy images taken at 1 week highlight for the 1SAliajMg3Nd_B_CAHAp sample, on the external face of the calvaria after peeling off the integument, the formation of a rich fibrous connective tissue with a gelatinous appearance covering the sample. In the detail images, sample particles were observed in the repair connective tissue, in various stages from a looser structure to a gelatinous, fibrous structure. **Histological evaluation**

In the case of the biological samples collected from batch 1S Mg3Nd_A, the areas of residual alloy delimited by connective tissue can be observed near a bone edge. For the biological samples collected from batch 1S Mg3Nd_B, the concentric arrangement around the alloy fragments of a connective tissue rich in cells is observed, especially around the disintegrated particles, cells with a rich metabolic activity evidenced by the presence of large nuclei, areas of cellular tissue with macrophage activity being delimited by connective fibers with a loose appearance (Figure 6.42.).

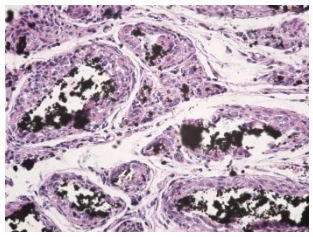

Figure 6.42. Appearance of a biological sample collected from lot 1S Mg3Nd_B, Col HE 20x

The samples analyzed generally showed good biocompatibility, with no detectable systemic manifestations in the laboratory animals used and with reduced local clinical inflammatory manifestations. In general, we noticed a great inter-individual variability related to the speed of evolution of the degradation process of the magnesium samples/alloys and the formation and maturation of the repair connective tissue, but also the coexistence of different evolutionary stages within the same case, without being able to make judgments specific to a single batch. In the batches where the laboratory animals were sacrificed one week after the alloy insertion, the inserted sample was always found in a volume of 50-80% of the initial volume (50% of the initial volume for the MG3Nd_A and Mg3Nd_B alloy samples and respectively 80% for the Mg3Nd_A_CAHAp and Mg3Nd_B_CAHAp samples), while in the samples collected after three weeks fragmented dispersed from the initial sample and an impregnation of the sample particles in the adjacent biological structures without affecting their functionality were identified.

ConCluSIonS

C1. General conclusions

➢ In the theoretical part of the thesis, an extensive literature study was carried out on the current state of research on the types and properties of magnesium and its alloys, as well as on the types of magnesium alloys used in medicine, as well as on the methods of modifying the surfaces of degradable biomaterials used in making orthopedic implants.

➢ Magnesium alloys present, compared to the metallic biomaterials that have been used until now for the execution of orthopedic implants (stainless steels and titanium alloys), several advantages because they are biodegradable, biocompatible and have mechanical properties similar to those of bone tissue. However, the too rapid degradation of commercial magnesium alloys as a result of their corrosion in the human body limits their clinical applicability because a high degradation rate causes premature deterioration of their functionality in the human body.

➢ Literature studies have shown that magnesium alloys stimulate the formation and growth of new bone tissue, due to the fact that magnesium is found in the composition of bone tissue and intervenes in metabolic processes. For this reason, there are many studies and research related to the use of magnesium alloys in the execution of implants for orthopedic and trauma surgery.

➢ Following the complex literature study carried out, it was demonstrated that magnesium alloys containing chemical elements from the category of rare earths, zinc and zirconium have a good potential to be used in the execution of biodegradable orthopedic implants. It is considered that Nd should be used as the main alloying element due to the optimal combination of excellent solubility in solid solution, market availability and its cost.

➢ Studies and research on polymer coatings of biodegradable magnesium alloys, with a role in reducing and controlling the rate of degradation, are a very current topic. Great variety of methods used in obtaining polymer coatings and the fact that the phenomena that take place are not fully elucidated, support the fact that every contribution made in this field will add to the development of this research direction.

➢ The properties of the polymer layer deposited on biodegradable magnesium alloys and its adhesion to the substrate depend on the method selected in making the coating and the working conditions.

➢ Following the literature study carried out, an advantageous method in terms of the uniformity of the deposited layer and the adhesion of the layer to the substrate is the method of immersion in a solution based on cellulose acetate with and without hydroxyapatite or magnesium particles.

C2. Original contributions

➢ The degradation behavior of magnesium alloys and their corrosion rate also depend on their surface properties. The influence of processing parameters and implant geometry on the functional properties and behavior of orthopedic implants during degradation are still being investigated.

➢ In the development of new magnesium alloys used for the production of biodegradable orthopedic implants, properties such as biocompatibility and corrosion resistance must be considered as the first requirements because the degradation of the implants must not affect the biological functions of the body.

➢ Currently, to reduce the corrosion rate of magnesium alloys, several technological possibilities are used, namely the addition of alloying elements and the deposition of biocompatible layers, such as bioresorbable polymers because they have good compatibility with bone tissue.

➢ The main objective of the experimental research was to determine the influence of the reinforcing elements on the structural, morphological characteristics, chemical composition, swelling rate and degradation rate of composite coatings with polymer matrix based on cellulose acetate.

➢ Another objective of the experimental research was to determine the effect of the composite coatings on the structural, morphological characteristics and functional properties of the magnesium alloy samples.

➢ A complex characterization of the structure of the alloys in the Mg3Nd system (Mg3Nd_A and Mg3Nd_B) was performed by optical microscopy, scanning electron microscopy (SEM) coupled with EDS spectrometry and X-ray diffraction (XRD).

➢ Four different types of coatings were obtained, a control sample made of cellulose acetate, a sample based on cellulose acetate and HAp particle reinforcement, a sample based on cellulose acetate and Mg particle reinforcement and a sample based on cellulose acetate and reinforcing elements HAp particles and Mg particles.

➢ The hydroxyapatite and magnesium particles used in obtaining the polymer coatings were analyzed by SEM, EDS, FT-IR, XRD.

➢ In the case of the coatings, scanning electron microscopy (SEM) was used to evaluate the surface properties, energy dispersive X-ray spectroscopy (EDS) was used to evaluate the elemental composition, and Fourier transform infrared spectroscopy was used to evaluate the structural characteristics (FT-IR) and RAMAN spectroscopy. Thermogravimetric analysis was also performed, the swelling rate and the degradation rate of the coatings were determined. The biocompatibility of the obtained coatings was evaluated by the MTT test and the cell viability test with Calcein-AM.

➢ Four types of coated magnesium alloy samples were obtained by the immersion method: Mg3Nd_A alloy with HAp composite coating, Mg3Nd_A alloy with Mg composite coating, Mg3Nd_B alloy with HAp composite coating and Mg3Nd_B alloy with Mg composite coating.

➢ The evaluation of the surface properties of coated and uncoated Mg3Nd alloys was performed by scanning electron microscopy (SEM), by determining the contact angle and roughness parameters.

➢ Functional testing of both Mg3Nd magnesium alloys and Mg3Nd magnesium alloys coated with a composite polymer layer was performed to evaluate the biodegradation and

corrosion resistance by determining the amount of hydrogen released, immersion tests and electrochemical tests, in the SBF solution.

➢ The results showed that the polymer coating with hydroxyapatite particles leads to the reduction of the corrosion rate, regardless of the type of alloy in the Mg3Nd system used as a substrate.

➢ In vivo and in vitro biocompatibility evaluation tests were performed. The in vitro evaluation of biocompatibility was performed on the polymer coatings obtained by the MTT test and the cell viability test with Calcein-AM. In vivo biocompatibility evaluation was performed for uncoated and coated Mg3Nd alloys with a composite polymer layer with hydroxyapatite particles using laboratory rats, Whistar breed. In vitro cytotoxicity tests demonstrated that polymer coatings composited with HAp or Mg particles are biocompatible and can be used to coat magnesium alloys. The in vivo tests showed for the batches where the laboratory animals were sacrificed one week after the alloy insertion that the inserted sample was always found in a volume of 50-80% of the initial volume (50% of the initial volume for the samples of alloy Mg3Nd_A and Mg3Nd_B and respectively 80% for the Mg3Nd_A_CAHAp and Mg3Nd_B_CAHAp samples), while in the samples collected at three weeks fragmented dispersed from the initial sample and an impregnation of the sample particles in the adjacent biological structures without affecting their functionality were identified. On the studied histological slides it was possible to identify the specific morphological aspects of 124 cell types varying from undifferentiated mesenchymal cells and fibroblasts in the repair tissue to polymorphonuclear neutrophils, monocytes and macrophages near the sample fragments

➢ The studies carried out allow us to conclude that the main objective of the doctoral thesis was fulfilled, namely the potential of Mg3Nd alloys with different Y content (Mg3Nd_A and Mg3Nd_B) to be usable in the execution of osteosynthesis implants was evaluated. It was also demonstrated the positive effect induced by the coating of these alloys with composite polymer coatings with HAp particles, by the immersion method, on their biodegradation and biocompatibility characteristics.

➢ I mention the fact that the experimental part was carried out mainly in the laboratories of the Department of Metallic Materials Science and Physical Metallurgy, Faculty of Materials Science and Engineering, National University of Science and Technology Polytechnic of Bucharest, but experimental determinations were also carried out in other laboratories. The in vitro biocompatibility evaluation tests were performed at the University of Medicine and Pharmacy Grigore T. Popa Iași, Faculty of Medical Bioengineering, and the in vivo biocompatibility evaluation tests at the Craiova University of Medicine and Pharmacy Biobase.

C3. Prospects for further development

This doctoral thesis has prospects for further development in several directions.

➢ It is possible to expand the studies regarding the functionality of experimental magnesium alloys from the Mg3Nd system by performing complex mechanical tests, on experimental samples in different stages of degradation, as a result of immersion in simulated biological fluids;

➢ Other cellulose acetate-based composite coatings can be made for the functionalization of biodegradable magnesium alloys, by adding growth factors or drugs with an antibacterial role;

➢ Experimental research can also be extended by in vivo biofunctionality testing in specific animal models to assess the degree of bone fracture repair.

➢ The role played by composite coatings in terms of the evolution of degraded surfaces in terms of surface compounds and osseointegration can also be evaluated more precisely in the case of animal model biofunctionality tests.

VALUATION OF RESEARCH RESULTS

Articles in ISI indexed and rated journals in the field of the PhD thesis

1.**Streza, A**.; Antoniac, A.; Manescu, V.; Paltanea, G.; Robu, A.; Dura, H.; Verestiuc, L.; Stanica, E.; Voicu, SI; Antoniac, I.; et al.*Effect of Filler Types on Cellulose-Acetate-Based Composite Used as Coatings for Biodegradable Magnesium Implants for Trauma. Materials*, (Q1), 2023, 16, 554.

2. Fosca, M.;**Streza, A**.; Anthony, VI; Vadalà G.; Rau, JV.*; Ion-Doped Calcium Phosphate-Based Coatings with Antibacterial Properties*. Journal of Functional Biomaterials, (Q1), 2023, 14(5), 1-44.

3. Dragomir (Nicolescu), L.; Anthony, VI; Manescu (Paltanea), V.; Antoniac, A.; Miculescu, M.; Trante, O.;**Streza, A**.; Furnace, YES*Microstructure and Corrosion Behavior of Mg-Ca and Mg-Zn-Ag Alloys for Biodegradable Hard Tissue Implants*. Crystals, (Q2), 2023, 13(8), 1213.

4.**Streza, A**.; Antoniac, A.; Manescu (Paltanea), V.; Ciocoiu, R.; Cotruț, CM; Miculescu, M.; Miculescu, F.; Anthony, VI; Fosca, M.; Rau, JV; Dura, H.*In vitro studies regarding the effect of cellulose acetate-based composite coatings on the functional properties of the biodegradable Mg3Nd alloys*, Biomimetics, 2023 (under review).

Participation in international conferences:

E1.**Alexander Streza**, Antoniac Aurora, Alina Robu, Diana Popescu, Voicu Stefan, Robert Ciocoiu, Antoniac Iulian - Characterization of the polylactic acid for magnesium alloys - 9th International Conference "Biomaterials, Tissue Engineering & Medical Devices" BIOMMEDD'2022, Bucharest, Romania

E2.**Alexander Streza**, Iulian Antoniac, Voicu Stefan, Aurora Antoniac, Alina Robu, Robert Ciocoiu - Characterization of the cellulose acetate coatings for magnesium alloys - Biomaterials and Novel Technologies for Healthcare, BIOMAH 2022, Rome, Italy

E3. Andrei Scripcaru, Paul Dan Sirbu, Robert Ciocoiu, Ramona Turcu, Octavian Trante, Iulian Antoniac, Alina Robu,**Alexander Streza**-A wetting study on the surface of stressed humerus fixation plates - 9th International Conference on Materials Science and Technologies – RoMat 2022, Bucharest, Romania

E4. Iulian Spanu, Aurora Antoniac, Alina Robu, Daniela Gheorghiță,**Alexander Streza**, Iulian Antoniac - Antimicrobial Copper - Based Coatings: Potential Biomedical Applications - 9th International Conference on Materials Science and Technologies – RoMat 2022, Bucharest, Romania

E5. Iulian Spanu, Aurora Antoniac, Alina Robu,**Alexander Streza**, Iulian Antoniac Surface properties for the thermal spray copper-based coatings on different metallic alloys - International Conference BioReMed 2023, Sibiu, Romania 126

E6.**Alexander Streza**, Aurora Antoniac, Stefan IoanVoicu, Vasile Iulian Antoniac, Degradation and Biocompatibility Studies on Cellulose-Acetate-Based Composite used as Coatings for Biodegradable Magnesium Implants; oral presentation; 6th International Conference on Functional Materials -ICFM 2023, March 18-21, 2023, Hammamet, Tunisia.

E7.**Alexander Streza**, Iulian Antoniac, Veronica Păltânea, Robert Ciocoiu, Cosmin Nicolescu In vitro evaluation of corrosion behavior for two polymer-coated Mg-3Nd alloys - International Conference BioReMed 2023, Sibiu, Romania.

International scientific awards

Best Poster Award – Characterization of the cellulose acetate coatings for magnesium alloys - Biomaterials and Novel Technologies for Healthcare, BIOMAH 2022, Rome, Italy.

Index of figures

Index of tables

Selective Bibliography

3. Prakasam, M.; Locs, J.; Salma-Ancane, K.; Loca, D.; Largeteau, A.; Berzina-Cimdina, L. Biodegradable Materials and Metallic Implants—A Review. J Funct Biomater 2017, 8, 44, doi:10.3390/jfb8040044.

15. Antoniac, I.; Miculescu, M.; Dinu, M. Metallurgical Characterization of Some Magnesium Alloys for Medical Applications. Solid State Phenomena 2012, 188, 109–113, doi:10.4028/www.scientific.net/SSP.188.109.

47. Esmaily, M.; Svensson, JE; Fajardo, S.; Birbilis, N.; Frankel, GS; Virtanen, S.; Arrabal, R.; Thomas, S.; Johansson, LG Fundamentals and Advances in Magnesium Alloy Corrosion. Prog Mater Sci 2017, 89, 92–193, doi:10.1016/j.pmatsci.2017.04.011

49. Xin, Y.; Hu, T.; Chu, PK Influence of Test Solutions on In Vitro Studies of Biomedical Magnesium Alloys. J Electrochem Soc 2010, 157, C238, doi:10.1149/1.3421651.

50. Antoniac, I.; Miculescu, M.; Manescu (Păltânea), V.; Stere, A.; Quan, PH; Paltânea, G.; Robu, A.; Earar, K. Magnesium-Based Alloys Used in Orthopedic Surgery. Materials 2022, 15, 1148, doi:10.3390/ma15031148.

68. Burmester, A.; Willumeit-Römer, R.; Feyerabend, F. Behavior of Bone Cells in Contact with Magnesium Implant Material. J Biomed Mater Res B Appl Biomater 2017, 105, 165–179, doi:10.1002/jbm.b.33542.

69. Fischer, J.; Pröfrock, D.; Hort, N.; Willumeit, R.; Feyerabend, F. Improved Cytotoxicity Testing of Magnesium Materials. Materials Science and Engineering: B 2011, 176, 830–834, doi:10.1016/j.mseb.2011.04.008.

81. Hornberger, H.; Virtanen, S.; Boccaccini, AR Biomedical Coatings on Magnesium Alloys – A Review. Acta Biomater 2012, 8, 2442–2455, doi:10.1016/j.actbio.2012.04.012.

142. Neacsu, P.; Staras, A.; Voicu, S.; Ionascu, I.; Sun, T.; Uzun, S.; Cojocaru, V.; Pandele, A.; tailor, S.; Miculescu, F.; et al. Characterization and In Vitro and In Vivo Assessment of a Novel Cellulose Acetate-Coated Mg-Based Alloy for Orthopedic Applications. Materials 2017, 10, 686, doi:10.3390/ma10070686.

193. Heise, S.; Virtanen, S.; Boccaccini, AR Tackling Mg Alloy Corrosion by Natural Polymer Coatings—A Review. J Biomed Mater Res A 2016, 104, 2628–2641, doi:10.1002/jbm.a.35776.

218. Bairagi, D.; Mandal, S. A Comprehensive Review on Biocompatible Mg-Based Alloys as Temporary Orthopedic Implants: Current Status, Challenges, and Future Prospects. Journal of Magnesium and Alloys 2022, 10, 627–669, doi:10.1016/j.jma.2021.09.005.

238. Quan, PH; Antoniac, I.; Miculescu, F.; Antoniac, A.; Manescu, V.; Robu, A.; Bita, AI; Miculescu, M.; Saceleanu, A.; Bodog, AD; et al. Fluoride Treatment and In Vitro Corrosion Behavior of Mg-Nd-Y-Zn-Zr Alloys Type. Materials 2022, 15, doi:10.3390/ma15020566

245. Abdal-hay, A.; Dewidar, M.; Lim, JK Biocorrosion Behavior and Cell Viability of Adhesive Polymer Coated Magnesium Based Alloys for Medical Implants. Appl Surf Sci 2012, 261, 536–546, doi:10.1016/j.apsusc.2012.08.051.

266. Mareci, D.; Bolat, G.; Izquierdo, J.; Crime, C.; Munteanu, C.; Antoniac, I.; Souto, RM Electrochemical Characteristics of Bioresorbable Binary MgCa Alloys in Ringer's Solution: Revealing the Impact of Local PH Distributions during in-Vitro Dissolution. Materials Science and Engineering: C 2016, 60, 402–410, doi:10.1016/j.msec.2015.11.069.

271. Zemková, M.; Minárik, P.; Dittrich, J.; Bohlen, J.; Král, R. Individual Effect of Y and Nd on the Microstructure Formation of Mg-Y-Nd Alloys Processed by Severe Plastic Deformation and Their Effect on the Subsequent Mechanical and Corrosion Properties. Journal of Magnesium and Alloys 2023, 11, 509–521, doi:10.1016/j.jma.2023.01.012.